Angewandte Chemie
Eine Zeitschrift der Gesellschaft Deutscher Chemiker

Supporting Information

The 9*H*-9-Borafluorene Dianion: A Surrogate for Elusive Diarylboryl Anion Nucleophiles

Jannik Gilmer[+], *Hendrik Budy*[+], *Thomas Kaese, Michael Bolte, Hans-Wolfram Lerner, and Matthias Wagner**

anie_201914219_sm_miscellaneous_information.pdf

Table of contents

1. Experimental details and characterization data

General considerations: All reactions, manipulations, and analyses were carried out under an atmosphere of dry argon in a glovebox or by applying standard Schlenk techniques. THF, Et_2O, and C_6H_6 were dried over Na/benzophenone; [D_8]THF was dried over Na-K alloy without benzophenone (2-3 d). Prior to use, the solvents were distilled from the drying agent and then degassed by applying three freeze-pump-thaw cycles. Me_3SiCl and Et_3SiCl were dried over CaH_2 and also degassed by applying three freeze-pump-thaw cycles prior to use. 4-Chloro-1-butene and 1-bromo-1-butene were degassed by applying three freeze-pump-thaw cycles prior to use. Compound $(\mathbf{1})_2$[S1] and the reference compound **4**[S2] were synthesized according to literature procedures.

NMR spectra were recorded at 298 K using Bruker Avance II 300, Avance III 500 HD, or DRX 600 spectrometers. Chemical shift values are referenced to (residual) solvent signals (^{1}H/^{13}C{^{1}H}; [D_8]THF: δ = 3.58/67.21 ppm[S3]) or external LiCl in D_2O (^{7}Li), $BF_3{\cdot}Et_2O$ (^{11}B/^{11}B{^{1}H}), and $SnMe_4$ + 5% C_6D_6 (^{119}Sn{^{1}H}). Abbreviations: s = singlet, d = doublet, t = triplet, q = quartet, br = broad, n.r. = multiplet expected in the ^{1}H NMR spectrum but not resolved. Resonances of carbon atoms attached to boron atoms were typically broadened and sometimes only observed in ^{1}H-^{13}C-HMBC experiments due to the quadrupolar relaxation of boron. The alkali metal salts M_2[**1**] and M_2[**2**] are formed as THF solvates, which were typically dried in a dynamic vacuum (oil pump; approximately 10^{-3} torr, room temperature, 10 to 20 min). After this drying process, the number of remaining THF ligands typically varies between individual samples and with respect to the THF content of corresponding single-crystalline material (cf. the X-ray crystal structure analyses). It is therefore advisable to determine the individual THF content of each sample by means of ^{1}H NMR spectroscopy.

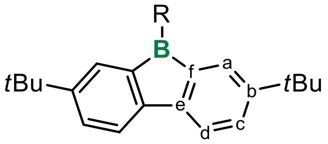

Figure S1. Numbering scheme used for the assignment of the ^{1}H and ^{13}C{^{1}H} NMR resonances.

1.1 Synthesis of M_2[1] (M = Li, Na, K)

Synthesis of Li_2[1]: $(\mathbf{1})_2$ (120 mg, 217 μmol, 1 equiv) was dissolved in THF (1.5 mL) to furnish a solution of 2 equiv of **1**·THF.[S4] In a separate Schlenk flask, lithium granules (49 mg, 7.1

mmol, 33 equiv) were covered with THF (2.0 mL) and cooled to –78 °C. The solution of **1**·THF was added dropwise over a period of 10 min, whereupon the reaction mixture adopted a dark green color. The reaction mixture was stirred at –78 °C for 1 h and at room temperature overnight. The dark greenish-brown solution was separated from residual lithium metal *via* syringe. All volatiles were removed under reduced pressure to afford Li_2[**1**] as a greenish-brown solid. Molecular formula of the *in vacuo* dried solvate complex, according to ^{1}H NMR spectroscopy: [Li_2(thf)$_{2.5}$][**1**]. Yield: 191 mg (406 μmol, 94%).

Single crystals of [Li_2(thf)$_3$][**1**] were grown from a solution of Li_2[**1**] in THF/Et_2O (1:1) at –30 °C.

^{1}H NMR (500.2 MHz, [D$_8$]THF): δ = 7.93 (d, ^3J(H,H) = 8.6 Hz, 2H; H-d), 7.76 (d, ^4J(H,H) = 1.9 Hz, 2H; H-a), 6.39 (dd, ^3J(H,H) = 8.6 Hz, ^4J(H,H) = 1.9 Hz, 2H; H-c), 4.43 (br, 1H; BH), 1.39 ppm (s, 18H; CH_3).

^{7}Li NMR (194.4 MHz, [D$_8$]THF): δ = –7.9 ppm (s).

^{11}B NMR (160.5 MHz, [D$_8$]THF): δ = 3.7 ppm ($h_{1/2} \approx$ 290 Hz).

^{13}C{^{1}H} NMR (125.8 MHz, [D$_8$]THF): δ = 133.6 (C-b), 131.3 (br, C-f), 125.3 (C-a), 120.6 (C-d), 114.7 (C-e), 108.5 (C-c), 34.9 (C(CH_3)), 32.4 ppm (CH_3).

Synthesis of Na_2[1]: (**1**)$_2$ (50 mg, 91 μmol, 1 equiv) was dissolved in THF (1.5 mL) to furnish a solution of 2 equiv of **1**·THF.[S4] In a separate Schlenk flask, sodium metal (85 mg, 3.7 mmol, 41 equiv) was covered with THF (1.0 mL) and cooled to –78 °C. The solution of **1**·THF was added dropwise over a period of 20 min, whereupon the reaction mixture adopted a dark green color. The reaction mixture was stirred at –78 °C for 1 h and at room temperature for 1 d.[S5] The dark green solution was separated from residual sodium metal *via* syringe. All volatiles were removed under reduced pressure to afford Na_2[**1**] as a greenish-brown solid. Molecular formula of the *in vacuo* dried solvate complex, according to ^{1}H NMR spectroscopy: [Na_2(thf)$_{4.5}$][**1**]. Yield: 117 mg (181 μmol, 99%).

Single crystals of [Na(thf)$_3$][Na(thf)][**1**] were grown from a solution of Na_2[**1**] in THF/Et_2O (1:1) at –30 °C.

^{1}H NMR (500.2 MHz, [D$_8$]THF): δ = 7.83 (d, ^3J(H,H) = 8.3 Hz, 2H; H-d), 7.81 (d, ^4J(H,H) = 1.9 Hz, 2H; H-a), 6.18 (dd, ^3J(H,H) = 8.3 Hz, ^4J(H,H) = 1.9 Hz, 2H; H-c), 4.46 (br, 1H; BH), 1.35 ppm (s, 18H; CH_3).

^{11}B NMR (160.5 MHz, [D$_8$]THF): δ = 3.9 ppm ($h_{1/2} \approx$ 290 Hz).

^{13}C{^{1}H} NMR (125.8 MHz, [D$_8$]THF): δ = 134.9 (br; C-f), 131.5 (C-b), 123.9 (C-a), 119.4 (C-d), 118.1 (C-e), 104.3 (C-c), 34.9 (*C*(CH$_3$)), 32.7 ppm (CH$_3$).

Synthesis of K$_2$[1]:

Method A: (**1**)$_2$ (106 mg, 192 µmol, 1 equiv) was dissolved in THF (1.5 mL) to furnish a solution of 2 equiv of **1**·THF.[S4] In a separate Schlenk flask, potassium metal (494 mg, 12.6 mmol, 66 equiv) was covered with THF (2.0 mL) and cooled to –78 °C. The solution of **1**·THF was added dropwise over a period of 10 min, whereupon the reaction mixture adopted a yellowish-brown color. The reaction mixture was stirred at –78 °C for 1 h and at room temperature overnight. The resulting reddish-brown solution was separated from residual potassium metal *via* syringe. All volatiles were removed under reduced pressure to afford K$_2$[**1**] as a brown solid. Molecular formula of the *in vacuo* dried solvate complex, according to ^{1}H NMR spectroscopy: [K$_2$(thf)][**1**]. Yield: 163 mg (382 µmol, 99%).

Method B: (**1**)$_2$ (100 mg, 181 µmol, 1 equiv) was dissolved THF (7.0 mL) to furnish a solution of 2 equiv of **1**·THF.[S4] In a separate Schlenk flask, KC$_8$ (733 mg, 5.42 mmol, 30 equiv) was covered with THF (3.0 mL). The solution of **1**·THF was added in one portion with stirring at room temperature to the KC$_8$ suspension, the mixture stirred for 1.5 h, and the resulting brown suspension filtered by using a frit (G3). The separated KC$_8$/graphite was washed with THF (3 × 0.5 mL) and the combined solutions were evaporated to dryness under reduced pressure to afford K$_2$[**1**] as a brown solid containing minor (approx. 20%) impurities of K$_2$[**2**] and K[**1H**] (according to NMR spectroscopy).

^{1}H NMR (500.2 MHz, [D$_8$]THF): δ = 7.73 (d, ^{3}J(H,H) = 8.2 Hz, 2H; H-d), 7.66 (n.r., 2H; H-a), 6.10 (dd, ^{3}J(H,H) = 8.2 Hz, ^{4}J(H,H) = 1.9 Hz, 2H; H-c), 4.34 (br, 1H; BH), 1.34 ppm (s, 18H; CH$_3$).

^{11}B NMR (160.5 MHz, [D$_8$]THF): δ = 8.0 ppm ($h_{1/2} \approx$ 360 Hz).

^{13}C{^{1}H} NMR (125.8 MHz, [D$_8$]THF): δ = 137.7 (br; C-f), 131.0 (C-b), 123.6 (C-a), 119.9 (C-e), 118.6 (C-d), 103.1 (C-c), 34.9 (*C*(CH$_3$)), 32.9 ppm (CH$_3$).

1.2 Reactivities of M$_2$[1] (M = Li, Na, K)

Synthesis of Li$_2$[2]: [Li$_2$(thf)$_{2.5}$][**1**] (210 mg, 446 µmol, 1.0 equiv) was dissolved in THF (5.0 mL) and cooled to –78 °C. (**1**)$_2$ (123 mg, 223 µmol, 0.5 equiv) was dissolved in THF (3.0 mL) to furnish a solution of 1.0 equiv of **1**·THF[S4] and added dropwise with stirring over a period of 45 min to the cold solution of Li_2[**1**]. Stirring was continued while the reaction mixture was slowly warmed to room temperature overnight. The solution was evaporated to dryness under reduced pressure. NMR spectroscopy revealed the quantitative formation of Li_2[**2**]. Molecular formula of the *in vacuo* dried solvate complex, according to ^{1}H NMR spectroscopy: [Li_2(thf)$_4$][**2**]. Yield: 378 mg (442 µmol, 99%).

Li_2[**2**] was recrystallized from a THF solution at –30 °C.

^{1}H NMR (300.0 MHz, [D$_8$]THF): δ = 7.24 (d, ^3J(H,H) = 7.9 Hz, 4H; H-d), 6.96 (n.r., 4H; H-a), 6.71 (dd, ^3J(H,H) = 7.9 Hz, ^4J(H,H) = 2.0 Hz, 4H; H-c), 2.1* (br, 2H; BH), 1.23 ppm (s, 36H; CH_3). *) This signal was detected through an ^{1}H{^{11}B} NMR experiment.

^{11}B NMR (96.3 MHz, [D$_8$]THF): δ = –15.3 ppm (d, ^1J(B,H) = 71 Hz).

The reported NMR shift values are consistent with literature data.[S4]

Synthesis of Na_2[2]: [Na_2(thf)$_{2.5}$][**1**] (48 mg, 96 µmol, 1.0 equiv) was dissolved in THF (1.5 mL) and cooled to –78 °C. (**1**)$_2$ (26 mg, 48 µmol, 0.5 equiv) was dissolved in THF (1.0 mL) to furnish a solution of 1.0 equiv of **1**·THF[S4] and added dropwise with stirring over a period of 30 min to the cold solution of Na_2[**1**]. The reaction mixture was stirred for 1 h at –78 °C, warmed to room temperature, and subsequently stirred for 1 h. The solution was evaporated to dryness under reduced pressure. NMR spectroscopy revealed the quantitative formation of Na_2[**2**]. Molecular formula of the *in vacuo* dried solvate complex, according to ^{1}H NMR spectroscopy: [Na_2(thf)$_2$][**2**]. Yield: 70 mg (94 µmol, 98%).

Single crystals of [Na_2(thf)$_6$][**2**] were grown from a THF solution at –30 °C.

^{1}H NMR (500.2 MHz, [D$_8$]THF): δ = 7.16 (d, ^3J(H,H) = 7.9 Hz, 4H; H-d), 6.86 (n.r., 4H; H-a), 6.65 (dd, ^3J(H,H) = 7.9 Hz, ^4J(H,H) = 2.0 Hz, 4H; H-c), 2.64 (q, ^1J(B,H) = 74 Hz, 2H; BH), 1.20 ppm (s, 36H; CH_3).

^{11}B NMR (160.5 MHz, [D$_8$]THF): δ = –12.5 ppm (d, ^1J(B,H) = 74 Hz).

^{13}C{^{1}H} NMR (125.8 MHz, [D$_8$]THF): δ = 167.4* (C-f), 142.7 (C-e), 142.7 (C-b), 126.6 (C-a), 117.5 (C-d), 117.1 (C-c), 34.8 (*C*(CH_3)), 32.5 ppm (CH_3). *) This signal was detected through an ^{1}H-^{13}C-HMBC NMR experiment.

Synthesis of K_2[2]: [K_2(thf)$_{1.5}$][**1**] (42 mg, 90 µmol, 1.0 equiv) was dissolved in THF (2.0 mL) and cooled to –78 °C. (**1**)$_2$ (24 mg, 45 µmol, 0.5 equiv) was dissolved in THF (1.0 mL) to furnish a solution of 1.0 equiv of **1**·THF[S4] and added dropwise with stirring over a period of 50 min to the cold solution of K_2[**1**]. The reaction mixture was stirred for 80 minutes at –78 °C, warmed to room temperature, and subsequently stirred for 1h. The solution was evaporated to dryness under reduced pressure. NMR spectroscopy indicated the formation of K_2[**2**] as the main product with a selectivity of ≈60%. The side products are unknown.

^{1}H NMR (300.0 MHz, [D$_8$]THF): δ = 7.39 (br, 4H; H-a), 7.30 (d, ^3J(H,H) = 7.9 Hz, 4H; H-d), 6.72 (br d, ^3J(H,H) = 7.9 Hz, 4H; H-c), 2.9* (br, 2H; BH), 1.24 ppm (s, 36H; CH_3). *) This signal was detected through an ^{1}H{^{11}B} NMR experiment.

^{11}B NMR (96.3 MHz, [D$_8$]THF): δ = –14.1 ppm (d, ^1J(B,H) = 69 Hz).

^{13}C{^{1}H} NMR (125.8 MHz, [D$_8$]THF): δ = 175.4* (C-f), 144.0 (C-e), 143.1 (C-b), 128.1 (C-a), 117.1 (C-d), 116.6 (C-c), 35.0 (*C*(CH_3)), 32.6 ppm (CH_3). *) This signal was detected through an ^{1}H-^{13}C-HMBC NMR experiment.

Stepwise reduction of Na_2[2]: All manipulations described in this paragraph were performed in a glovebox. In a small Schlenk tube, [Na_2(thf)$_2$][**2**] (53 mg, 0.14 mmol, 1.0 equiv) was dissolved in [D$_8$]THF (0.7 mL); sodium metal (13 mg, 0.57 mmol, 7.8 equiv) was added at room temperature. After stirring for 2 h, the solution was separated from residual sodium metal by using a syringe and transferred to an NMR tube, equipped with a J. Young PTFE valve. After an ^{1}H NMR spectrum had been recorded, the solution was transferred back to the previously used flask (which still contained the residual sodium) using the same syringe. The reaction mixture was stirred for 4 h at room temperature before measuring a new ^{1}H NMR spectrum (following the procedure described above). This step was repeated three more times. Only in the last reduction step, the solution was stirred with sodium metal for 7 h at room temperature. NMR spectroscopy revealed the quantitative formation of Na_2[**1**], whereby the reduction progress forming 2 equiv of Na_2[**1**] out of Na_2[**2**] could be examined stepwise by the recorded ^{1}H NMR spectra.

Synthesis of Li[1Me]: [Li_2(thf)$_3$][**1**] (102 mg, 201 μmol, 1 equiv) was placed in a flask and dissolved in THF (4.0 mL). The solution was cooled to –196 °C and MeCl ((192 ± 9) μmol, 1 equiv) was condensed from a glass vessel onto the frozen solution. The amount of added MeCl was determined by measuring the pressure in the vessel by means of a mercury column (V = (66 ± 2) mL, p = (55 ± 2) mm Hg, T = (31 ± 1) °C) and applying the ideal gas law. The stirred solution was warmed to room temperature by using a water bath. The yellow solution was stirred for 45 min at room temperature and evaporated to dryness under reduced pressure. NMR spectroscopy revealed an essentially quantitative conversion to Li[**1Me**].

^{1}H NMR (500.2 MHz, [D$_8$]THF): δ = 7.48 (n.r., 2H; H-a), 7.31 (d, ^3J(H,H) = 7.8 Hz, 2H; H-d), 6.87 (dd, ^3J(H,H) = 7.8 Hz, ^4J(H,H) = 2.0 Hz, 2H; H-c), 2.20 (q, ^1J(B,H) = 75 Hz, 1H; BH), 1.32 (s, 18H; CH$_3$), –0.15 ppm (br s, 3H; BCH$_3$).

^{1}H{^{11}B} NMR (500.2 MHz, [D$_8$]THF): δ = 7.48 (n.r., 2H; H-a), 7.31 (d, ^3J(H,H) = 7.8 Hz, 2H; H-d), 6.87 (dd, ^3J(H,H) = 7.8 Hz, ^4J(H,H) = 2.0 Hz, 2H; H-c), 2.20 (q, ^3J(H,H) = 6.1 Hz, 1H; BH), 1.32 (s, 18H; CH$_3$), –0.15 ppm (d, ^3J(H,H) = 6.1 Hz, 3H; BCH$_3$).

^{11}B NMR (160.5 MHz, [D$_8$]THF): δ = –15.5 ppm (d, ^1J(B,H) = 75 Hz).

^{13}C{^{1}H} NMR (125.8 MHz, [D$_8$]THF): δ = 172.0 (q, ^1J(B,C) = 46 Hz; C-f), 146.6 (C-b), 144.6 (C-e), 127.4 (C-a), 119.1 (C-c), 116.9 (C-d), 34.8 (*C*(CH$_3$)), 32.4 (CH$_3$), 4.8 ppm (q, ^1J(B,C) = 41 Hz; BCH$_3$).

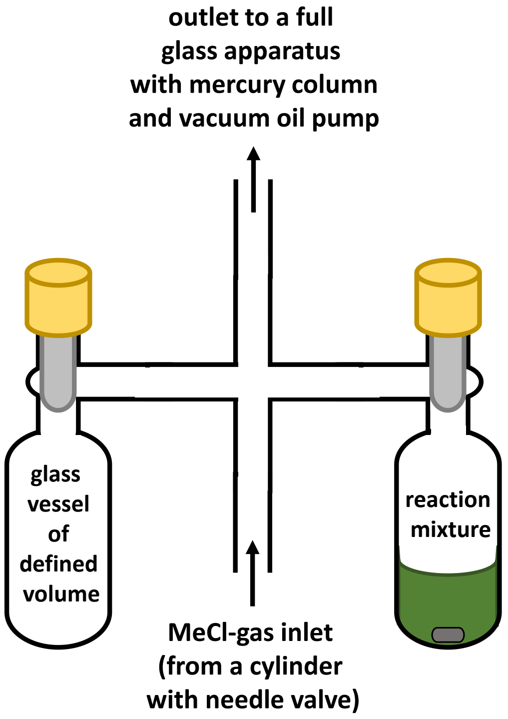

Figure S2: Schematic representation of the reaction apparatus for the condensation of the MeCl.

Targeted synthesis of an authentic sample of Li[1Me]: A solution of LiAlH$_4$ in Et$_2$O (1.0 M, 0.1 mL, 100 µmol, 3 equiv) was placed in an NMR tube. All volatiles were removed under reduced pressure. A solution of **4** (10 mg, 35 µmol, 1 equiv) in [D$_8$]THF was added in one portion to the NMR tube. Upon addition, an immediate discoloration of the formerly yellow solution was observed. NMR spectroscopy on the crude reaction mixture revealed an essentially quantitative conversion to Li[**1Me**]. The pure compound was obtained after extraction into C$_6$H$_6$.

Reaction of Li_2[1] with MeI

[$Li_2(thf)_{2.5}$][**1**] (10 mg, 21 µmol, 1 equiv) was dissolved in [D_8]THF (0.30 mL). MeI (1.3 µL, 21 µmol, 1 equiv) was diluted with [D_8]THF (0.20 mL) and the solution added dropwise with stirring at room temperature *via* syringe to the dark green solution of Li_2[**1**], whereupon the mixture instantaneously adopted a yellow color. NMR spectroscopy revealed the formation of a complex product mixture containing Li[**1Me**] (≈30%), Li[**1H**] (≈20%), Li_2[**2**] (≈10%), and Li[**3H**] (≈20%). The other side products are unknown.

Synthesis of 4:

Method A: [$Li_2(thf)_{2.5}$][**1**] (83 mg, 177 µmol, 1 equiv) was placed in a flask and dissolved in THF (4.0 mL). The solution was cooled to –196 °C and MeCl ((168 ± 9) µmol, 1 equiv) was condensed from a glass vessel onto the frozen solution. The amount of added MeCl was determined by measuring the pressure in the vessel by means of a mercury column (V = (51 ± 2) mL, p = (61 ± 2) mm Hg, T = (23 ± 1) °C) and applying the ideal gas law. The stirred solution was warmed to room temperature by using a water bath. The yellow solution was stirred for 15 min at room temperature and evaporated to dryness under reduced pressure. In a glovebox, the residue was dissolved in [D_8]THF (0.60 mL) and placed in a small screw-capped vial. Me_3SiCl (45 µL, 355 µmol, 2 equiv) was diluted with [D_8]THF (0.20 mL) and the solution added dropwise with stirring at room temperature *via* syringe to the yellow solution in the vial. Upon addition, no color change was observed. NMR-spectroscopy revealed an essentially quantitative conversion to **4** (>95% conversion, according to ^{1}H NMR spectroscopy) and Me_3SiH.

Method B: [$Li_2(thf)_{2.5}$][**1**] (20 mg, 43 µmol) was placed in an NMR-tube and dissolved in [D_8]THF (0.55 mL). The dark green solution was cooled to –196 °C, the tube was evacuated, warmed to room temperature, and flooded with MeCl (p = 1 atm). When the solution mixed with the gas, a discoloration was observed. The reaction mixture was cooled to –196 °C, the NMR tube evacuated, and flame sealed. NMR-spectroscopy revealed the formation of **4** (60% conversion, according to ^{1}H NMR spectroscopy) and CH_4. The side products are unknown.

^{1}H NMR (300.0 MHz, [D_8]THF): δ = 7.49 (d, ^4J(H,H) = 1.9 Hz, 2H; H-a), 7.37 (d, ^3J(H,H) = 7.9 Hz, 2H; H-d), 7.15 (dd, ^3J(H,H) = 7.9 Hz, ^4J(H,H) = 1.9 Hz, 2H; H-c), 1.32 (s, 18H; C(CH_3)) 0.30 ppm (s, 3H; BCH_3).

^{11}B NMR (96.3 MHz, [D_8]THF): δ = 11.9 ($h_{1/2}$ ≈ 520 Hz) ppm.

^{13}C{^{1}H} NMR (125.8 MHz, [D$_8$]THF): *δ* = 152.5 (br; C-f), 148.5 (C-b), 147.3 (C-e), 127.3 (C-a), 124.5 (C-c), 118.5 (C-d), 34.9 (*C*(CH$_3$)), 31.9 (CH$_3$), 3.2 ppm (br; BCH$_3$).

Byproduct Me$_3$SiH: ^{1}H NMR (300.0 MHz, [D$_8$]THF): *δ* = 3.95 (n.r., 1H; SiH), 0.07 (d, ^{3}J(H,H) = 3.7 Hz, 9H; CH$_3$). **^{13}C{^{1}H} NMR (125.8 MHz, [D$_8$]THF):** *δ* = –2.9 ppm.

Byproduct CH$_4$: ^{1}H NMR (500.2 MHz, [D$_8$]THF): *δ* = 0.18 ppm (s). **^{13}C{^{1}H} NMR (125.8 MHz, [D$_8$]THF):** *δ* = –4.6 ppm.

The reported NMR shift values of **4** and CH$_4$ are consistent with literature data.[S2, S3]

Synthesis of Li[1SiEt$_3$]: In the glovebox, [Li$_2$(thf)$_{2.5}$][**1**] (20 mg, 43 μmol, 1 equiv) was placed in a small screw-capped vial, dissolved in [D$_8$]THF (0.30 mL), and stirred. Et$_3$SiCl (7.1 μL, 43 μmol, 1 equiv) in [D$_8$]THF (0.20 mL) was added dropwise *via* syringe, whereupon the color of the reaction mixture changed from dark green to light green. NMR spectroscopy revealed an essentially quantitative conversion to Li[**1SiEt$_3$**] (>90% according to ^{1}H NMR spectroscopy).

^{1}H NMR (300.0 MHz, [D$_8$]THF): *δ* = 7.60 (br, 2H; H-a), 7.45 (d, ^{3}J(H,H) = 7.9 Hz, 2H; H-d), 6.87 (dd, ^{3}J(H,H) = 7.9 Hz, ^{4}J(H,H) = 2.0 Hz, 2H; H-c), 2.34 (q, ^{1}J(B,H) = 84 Hz, 1H; BH), 1.33 (s, 18H; CH$_3$), 0.70 (t,^{3}J(H,H) = 7.9 Hz, 9H; Si(CH$_2$C*H*$_3$)), 0.23 ppm (q, ^{3}J(H,H) = 7.9 Hz, 6H; Si(C*H*$_2$CH$_3$)).

^{11}B NMR (96.3 MHz, [D$_8$]THF): *δ* = –22.9 ppm (d, ^{1}J(B,H) = 84 Hz).

^{13}C{^{1}H} NMR (125.8 MHz, [D$_8$]THF): *δ* = 166.7 (q, ^{1}J(B,C) = 48 Hz; C-f), 145.9 (C-e), 143.8 (C-b), 128.1 (C-a), 117.7 (C-c), 117.4 (C-d), 34.8 (*C*(CH$_3$)), 32.4 (CH$_3$), 9.3 (Si(*C*H$_2$CH$_3$)), 5.9 ppm (Si(CH$_2$*C*H$_3$)).

The reported NMR shifts of Li[**1SiEt$_3$**] are consistent with literature data.[S6]

Synthesis of Li[1SnMe$_3$]: In the glovebox, [Li$_2$(thf)$_{2.5}$][**1**] (20 mg, 43 μmol, 1.0 equiv) was placed in a small screw-capped vial, dissolved in [D$_8$]THF (0.30 mL), and stirred. Me$_3$SnCl (8 mg, 40 μmol, 0.9 equiv)[S7] was separately dissolved in [D$_8$]THF (0.30 mL) and the solution added dropwise at room temperature *via* syringe to the dark green solution of Li$_2$[**1**], whereupon the mixture adopted a yellow color. NMR spectroscopy revealed the formation of Li[**1SnMe$_3$**] as the main product (≈80% conversion according to ^{1}H NMR spectroscopy and with reference to 0.9 equiv Me$_3$SnCl). The major side product is Li[**1H**]. In addition, traces of residual Li$_2$[**1**] were observed.

^{1}H NMR (500.2 MHz, [D$_8$]THF): δ = 7.55 (br, 2H; H-a), 7.44 (d, ^{3}J(H,H) = 7.8 Hz, 2H; H-d), 6.86 (dd, ^{3}J(H,H) = 7.8 Hz, ^{4}J(H,H) = 2.0 Hz, 2H; H-c), 2.81 (br, 1H; BH), 1.32 (s, 18H; CH$_3$), –0.48 ppm (s, ^{2}J($^{117/119}$Sn,H) = 31 Hz, 9H; Sn(CH$_3$)).

^{11}B NMR (160.5 MHz, [D$_8$]THF): δ = –19.5 ppm (br d, ^{1}J(B,H) = 87 Hz, ^{1}J(B,Sn) = 390 Hz).

^{13}C{^{1}H} NMR (125.8 MHz, [D$_8$]THF): δ = 165.6 (br; C-f), 144.9 (C-e), 144.2 (C-b), 127.9 (C-a), 117.9 (C-c), 117.4 (C-d), 34.7 (*C*(CH$_3$)), 32.3 (CH$_3$), –9.5 ppm (s, ^{1}J($^{117/119}$Sn,C) = 84 Hz; Sn(CH$_3$)).

^{119}Sn{^{1}H} NMR (186.5 MHz, [D$_8$]THF): δ = –44.0 ppm (q, ^{1}J(Sn,B) = 390 Hz).

Side product Sn$_2$Me$_6$: ^{1}H NMR (500.2 MHz, [D$_8$]THF): δ = 0.21 ppm (s, ^{2}J($^{117/119}$Sn,H) = 48 Hz, 18H). **^{119}Sn{^{1}H} NMR (186.5 MHz, [D$_8$]THF):** δ = –107.4 ppm (s, ^{1}J(^{117}Sn, ^{119}Sn) = 4290 Hz).

The reported NMR shift values of **Sn$_2$Me$_6$** are consistent with literature data.[S8, S9]

Reaction of Li$_2$[1] with the radical clock (bromomethyl)cyclopropane: [Li$_2$(thf)$_{2.5}$][**1**] (10 mg, 21 µmol, 1 equiv) was dissolved in [D$_8$]THF (0.30 mL). (Bromomethyl)cyclopropane (2.0 µL, 21 µmol, 1 equiv) was diluted with [D$_8$]THF (0.20 mL) and the solution added dropwise with stirring at room temperature *via* syringe to the dark green solution of Li$_2$[**1**], whereupon the mixture instantaneously adopted a yellow color. NMR spectroscopy revealed the formation of two main products. One of them was identified as Li$_2$[**2**]; the other one contained a tetracoordinate borafluorene fragment, a boron-bonded hydrogen atom, and an olefinic double bond. These observations are in accordance with the structure of Li[**1C$_2$H$_4$CH=CH$_2$)**] for the second main product (see below for additional evidence provided by an authentic sample; cf. Figure S3). As a third (minor) product, Li[**1H**] was detected.

Reaction of Li$_2$[1] with 4-bromo-1-butene: [Li$_2$(thf)$_{2.5}$][**1**] (15 mg, 32 µmol, 1 equiv) was dissolved in [D$_8$]THF (0.30 mL). 4-Bromo-1-butene (3.2 µL, 32 µmol, 1 equiv) was diluted with [D$_8$]THF (0.20 mL) and the solution added dropwise with stirring at room temperature *via* syringe to the dark green solution of Li$_2$[**1**], whereupon the mixture instantaneously adopted a yellow color. All major resonances in the ^{1}H NMR spectrum of the mixture are identical to those observed in the ^{1}H NMR spectrum recorded on the reaction mixture between Li$_2$[**1**] and (bromomethyl)cyclopropane (see Figure S45). Even the product distributions obtained from the reactions of Li$_2$[**1**] with (bromomethyl)cyclopropane and 4-bromo-1-butene are similar.

Synthesis of Li[$1C_2H_4CH{=}CH_2$]: In the glovebox, [$Li_2(thf)_{2.5}$][**1**] (10 mg, 21 µmol, 1.0 equiv) was placed in a small screw-capped vial, dissolved in [D_8]THF (0.30 mL), and stirred. 4-Chloro-1-butene (2.1 µL, 22 µmol, 1 equiv) was separately diluted in [D_8]THF (0.20 mL) and the solution added dropwise at room temperature *via* syringe to the dark green solution of Li_2[**1**], whereupon the mixture adopted a yellow color (the color change required approx. 30-60 seconds and was thus significantly slower than in the case of 4-bromo-1-butene). NMR spectroscopy revealed the formation of Li[$\mathbf{1C_2H_4CH{=}CH_2}$)] as the main product (≈75% conversion according to ^{1}H NMR spectroscopy). The major side products are Li[**1H**] and Li_2[**2**], but in this case, Li_2[**2**] is formed to a lesser extent than Li**[1H**].

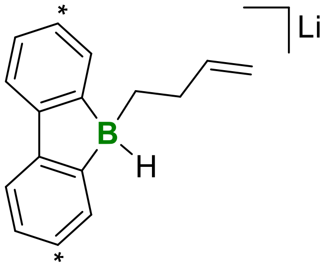

Li[$\mathbf{1C_2H_4CH{=}CH_2}$]

Figure S3: Structure of Li[$\mathbf{1C_2H_4CH{=}CH_2}$]. Carbon atoms marked with asterisks bear *t*Bu substituents.

^{1}H NMR (500.2 MHz, [D_8]THF): δ = 7.54 (br, 2H; H-a), 7.33 (d, ^3J(H,H) = 7.8 Hz, 2H; H-d), 6.90 (dd, ^3J(H,H) = 7.8 Hz, ^4J(H,H) = 2.0 Hz, 2H; H-c), 5.95 (ddt, ^3J(H,H) = 16.8 Hz, ^3J(H,H) = 10.0 Hz, ^3J(H,H) = 6.7 Hz, 1H; $CH_2CH_2CH{=}CH_2$), 4.76 (dm (^3J(H,H) = 16.8 Hz, 1H; $CH_2CH_2CH{=}CH_2$), 4.55 (dm (^3J(H,H) = 10.0 Hz, 1H; $CH_2CH_2CH{=}CH_2$), 2.15 (m, 2H, $CH_2CH_2CH{=}CH_2$), 2.11* (q, ^1J(B,H) = 76 Hz, 1H; BH), 1.32 (s, 18H; CH_3), 0.56 ppm (br, 2H, $CH_2CH_2CH{=}CH_2$).

* This signal gave a cross peak in an ^{1}H-^{11}B-HSQC NMR experiment.

^{11}B NMR (160.5 MHz, [D_8]THF): δ = –13.6 ppm (d, ^1J(B,H) = 76 Hz).

^{13}C{^{1}H} NMR (125.8 MHz, [D_8]THF): δ = 170.0 (C-f)*, 147.9 ($CH_2CH_2CH{=}CH_2$), 147.1 (C-e), 144.9 (C-b), 128.0 (C-a), 119.5 (C-c), 117.1 (C-d), 108.8 ($CH_2CH_2CH{=}CH_2$), 36.9 ($CH_2CH_2CH{=}CH_2$), 34.8 ($C(CH_3)$), 32.4 (CH_3), 24.5 ppm ($CH_2CH_2CH{=}CH_2$)*.

* This signal was detected through an ^{1}H-^{13}C-HMBC NMR experiment.

1.3 Mechanistic studies

Reduction of 1·THF at RT: (**1**)$_2$ (20 mg, 36 µmol, 1 equiv) was dissolved in [D_8]THF (0.65 mL) to furnish a solution of 2 equiv of **1**·THF. [S4] The yellow solution was treated with sodium metal (34 mg, 1.5 mmol, 42 equiv) and stirred for 1 d at room temperature. The resulting dark brown solution was separated from residual sodium metal *via* syringe. NMR spectroscopy revealed the formation of Na_2[**1**] (≈30%), Na_2[**3**] (≈15%) and Na[**1H**] (≈25%). The other side products are unknown.

Na_2[3]*:[S10] **^{1}H NMR (500.2 MHz, [D_8]THF):** δ = 9.27 (d, ^4J(H,H) = 2.2 Hz, 4H; H-a), 8.76 (d, ^3J(H,H) = 8.7 Hz, 4H; H-d), 7.14 (dd, ^3J(H,H) = 8.7 Hz, ^4J(H,H) = 2.2 Hz, 4H; H-c), 1.55 ppm (s, 36H; CH_3).
^{11}B NMR (96.3 MHz, [D_8]THF): δ = 32.0 ppm (vbr).

Na[1H]:[S10] **^{1}H NMR (500.2 MHz, [D_8]THF):** δ = 7.60 (br, 2H; H-a), 7.48 (d, ^3J(H,H) = 7.9 Hz, H; H-d), 7.03 (dd, ^3J(H,H) = 7.9 Hz, ^4J(H,H) = 1.8 Hz, 2H; H-c), 2.10 (q, ^1J(B,H) = 81 Hz, 2H; BH_2) 1.34 ppm (s, 18H; CH_3).
^{11}B NMR (160.5 MHz, [D_8]THF): δ = –23.1 ppm (t, ^1J(B,H) = 81 Hz).

*NMR signals were assigned using the same phenylene-ring numbering scheme as for borafluorene moieties with C^f bonded to boron, C^b bearing a *t*Bu-group and C^e bonded to a neighboring phenylene ring.

Reduction of 1·THF at only −78 °C: (**1**)$_2$ (50 mg, 91 μmol, 1 equiv) was dissolved in THF (1.5 mL) to furnish a solution of 2 equiv of **1**·THF.[S4] In a separate Schlenk flask, sodium metal (85 mg, 3.6 mmol, 40 equiv) was covered with THF (1.0 mL) and cooled to –78 °C. The solution of **1**·THF was added dropwise over a period of 20 min, whereupon the reaction mixture adopted a dark green color. The reaction mixture was stirred at –78 °C for 1 h, warmed to room temperature and the solution separated from residual sodium metal *via* syringe. The solution was evaporated to dryness under reduced pressure. NMR spectroscopy revealed the formation of Na_2[**1**] and Na_2[**2**] as the only products with a ratio of approx. 1:4.

Reaction of Na_2[2] with 1·THF: [$Na_2(thf)_2$][**2**] (12 mg, 16 μmol, 1.0 equiv) was dissolved in [D_8]THF (0.4 mL). (**1**)$_2$ (1 mg, 2 μmol, 0.13 equiv) was dissolved in [D_8]THF (0.2 mL) to furnish a solution of 0.25 equiv of **1**·THF[S4] and added dropwise with stirring *via* syringe. NMR spectroscopy revealed the formation of Na[**3H**] (≈7%) and Na[**1H**] (≈14%) as the main products.
Na[3H]*:[S10] **^{1}H NMR (300.0 MHz, [D_8]THF):** δ = 8.92 (d, ^4J(H,H) = 2.2 Hz, 4H; H-a), 8.51 (d, ^3J(H,H) = 8.7 Hz, 4H; H-d), 7.39 (dd, ^3J(H,H) = 8.7 Hz, ^4J(H,H) = 2.2 Hz, 4H; H-c), 1.51 ppm (s, 36H; CH_3).
^{11}B NMR (96.3 MHz, [D_8]THF): δ = n.o.

Note: The NMR signals of the *BHB* group are usually broadened and due to the low concentration of Na[**3H**] in the sample, these signals were not observed.[S4, S10]

*****NMR signals were assigned using the same phenylene-ring numbering scheme as for borafluorene moieties with C^f bonded to boron, C^b bearing a *t*Bu-group and C^e bonded to a neighboring phenylene ring.

2. Plots of the NMR spectra

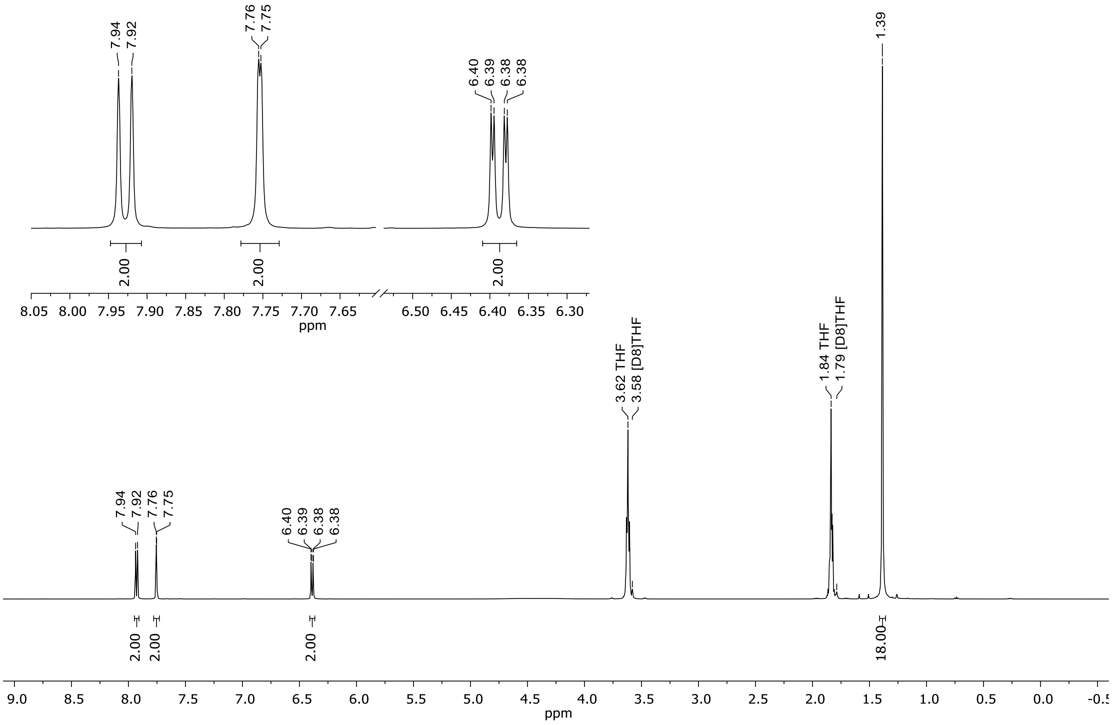

Figure S4: ^{1}H NMR spectrum of Li_2[**1**] (500.2 MHz, $[D_8]$THF).

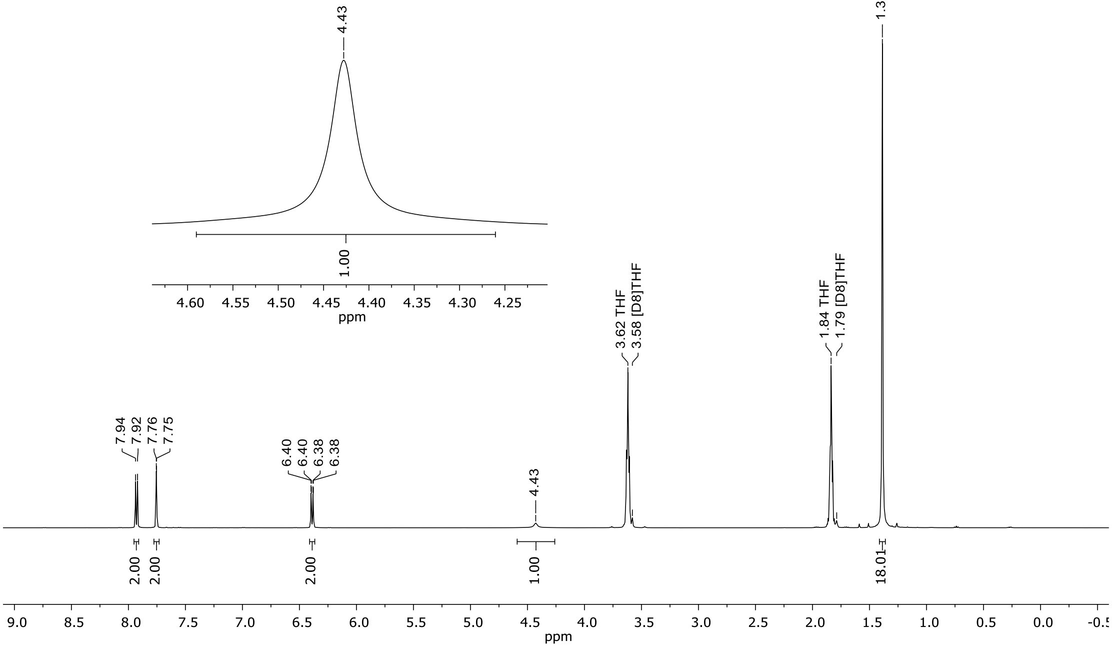

Figure S5: ^{1}H{^{11}B} NMR spectrum of Li_2[**1**] (500.2 MHz, $[D_8]$THF).

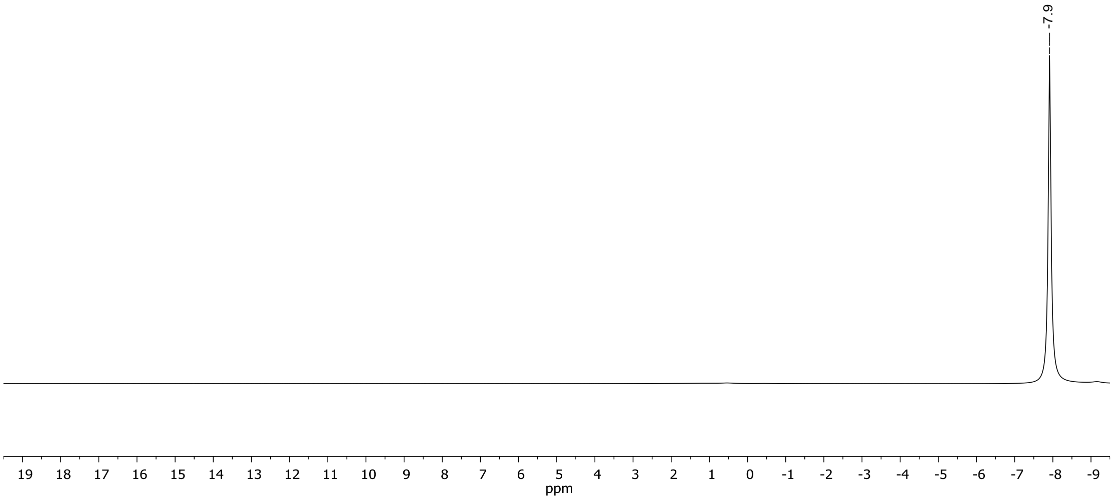

Figure S6: ^{7}Li NMR spectrum of Li$_2$[**1**] (194.4 MHz, [D$_8$]THF).

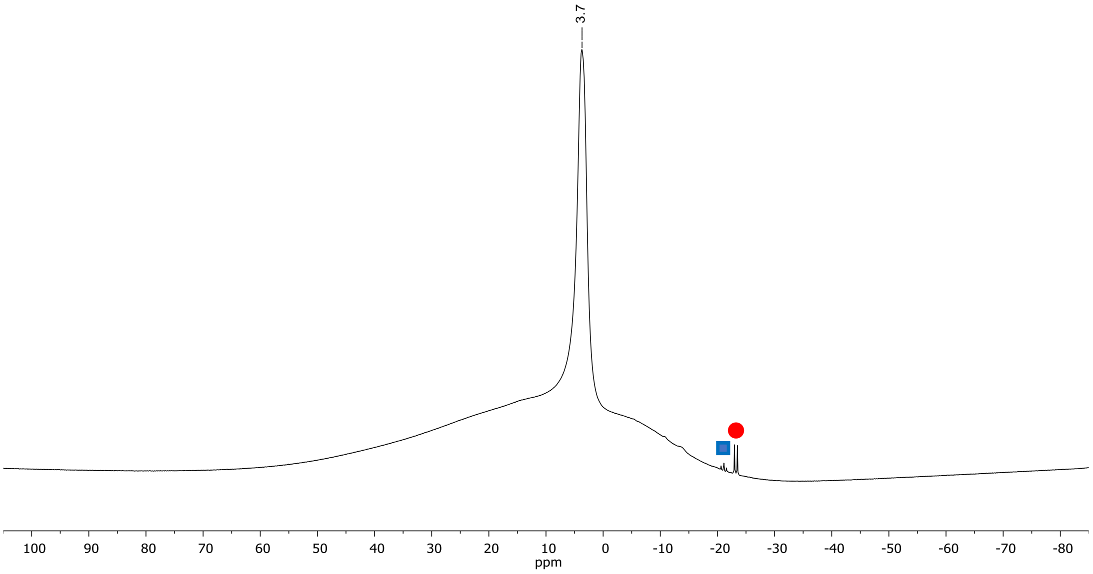

Figure S7: ^{11}B NMR spectrum of Li$_2$[**1**] (160.5 MHz, [D$_8$]THF). Observed minor components: Li[**1H**] (■, triplet), Li[**1SiEt$_3$**] (●, doublet).

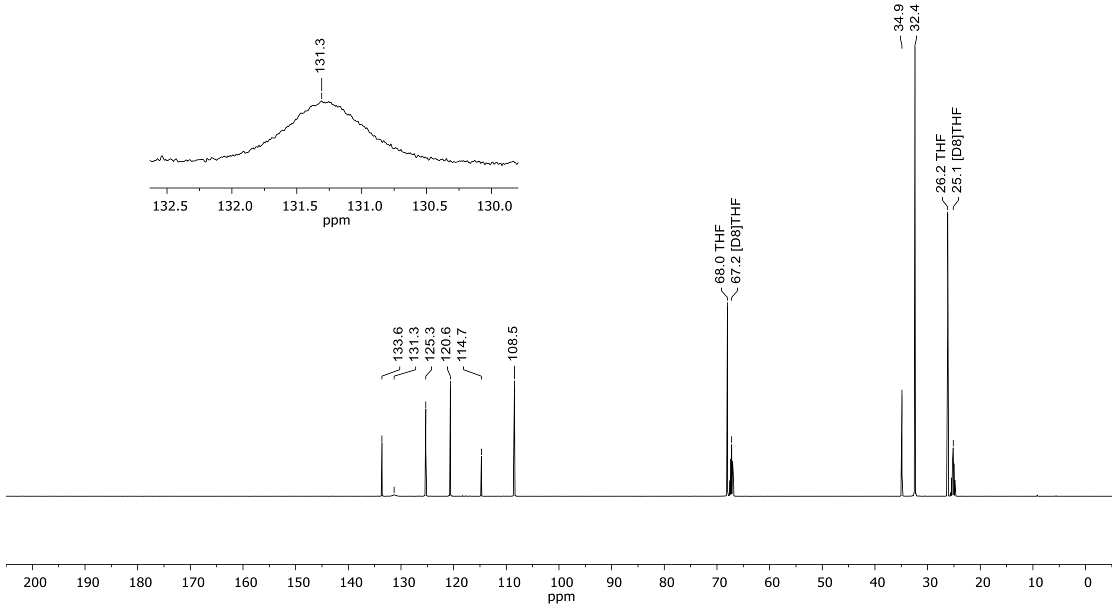

Figure S8: $^{13}C\{^1H\}$NMR spectrum of Li_2[**1**] (125.8 MHz, [D_8]THF).

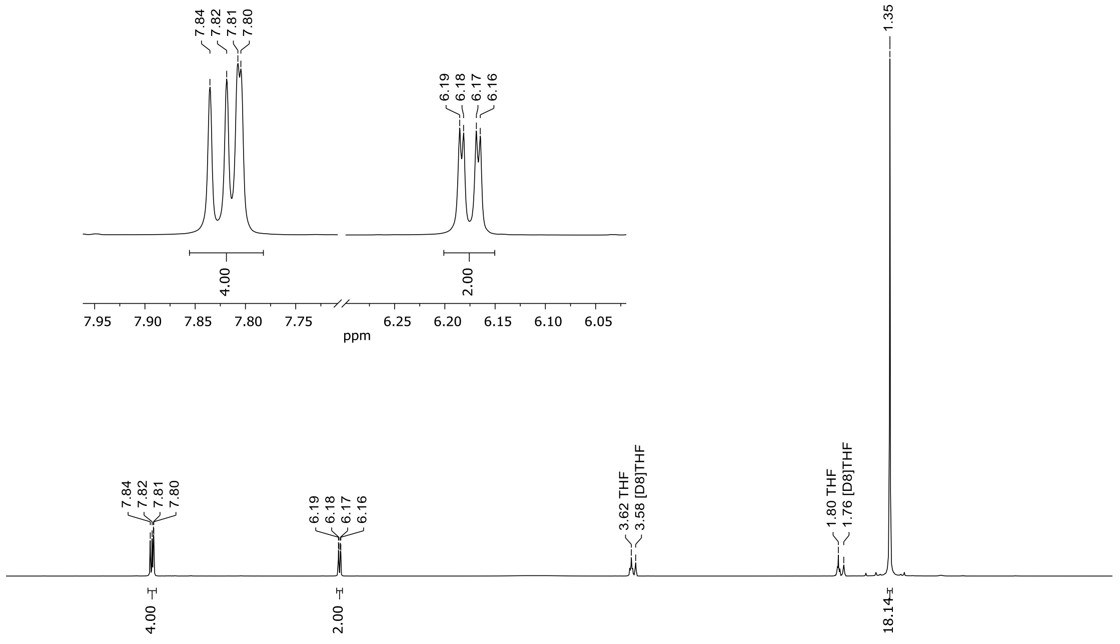

Figure S9: ^1H NMR spectrum of Na_2[**1**] (500.2 MHz, [D_8]THF).

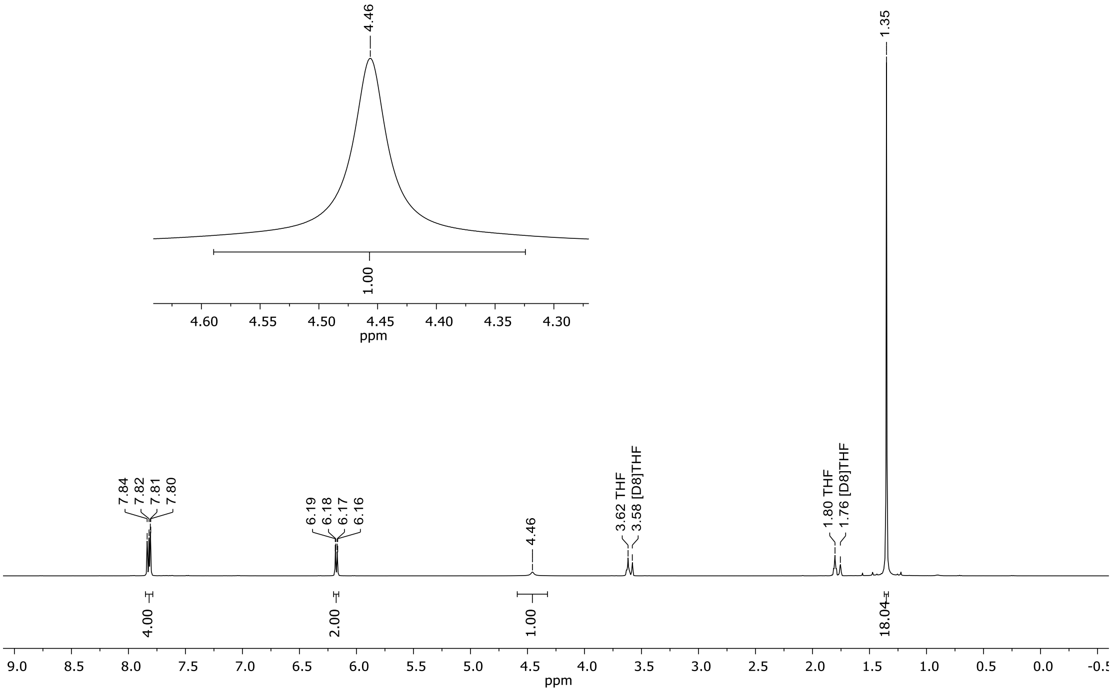

Figure S10: $^{1}H\{^{11}B\}$ NMR spectrum of Na_2[**1**] (500.2 MHz, [D_8]THF).

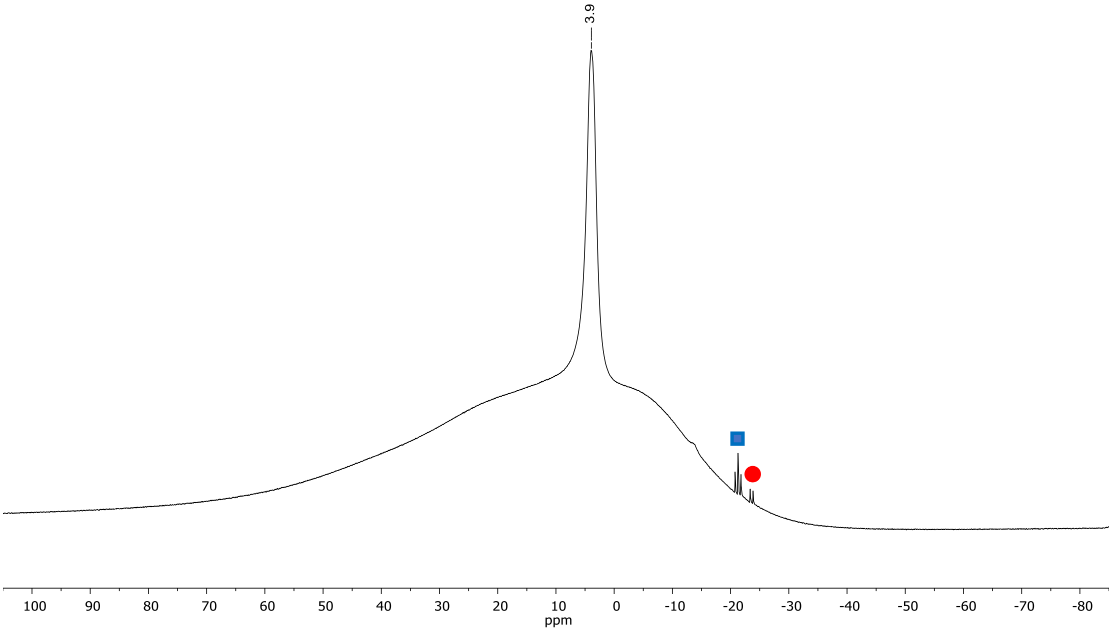

Figure S11: ^{11}B NMR spectrum of Na_2[**1**] (160.5 MHz, [D_8]THF). Observed minor components: Na[**1H**] (■, triplet; assigned by analogy with Li[**1H**][S10] and K[**1H**][S10]), Na[**1SiEt$_3$**] (●, doublet; assigned by analogy with Li[**1SiEt$_3$**][S6, S10]).

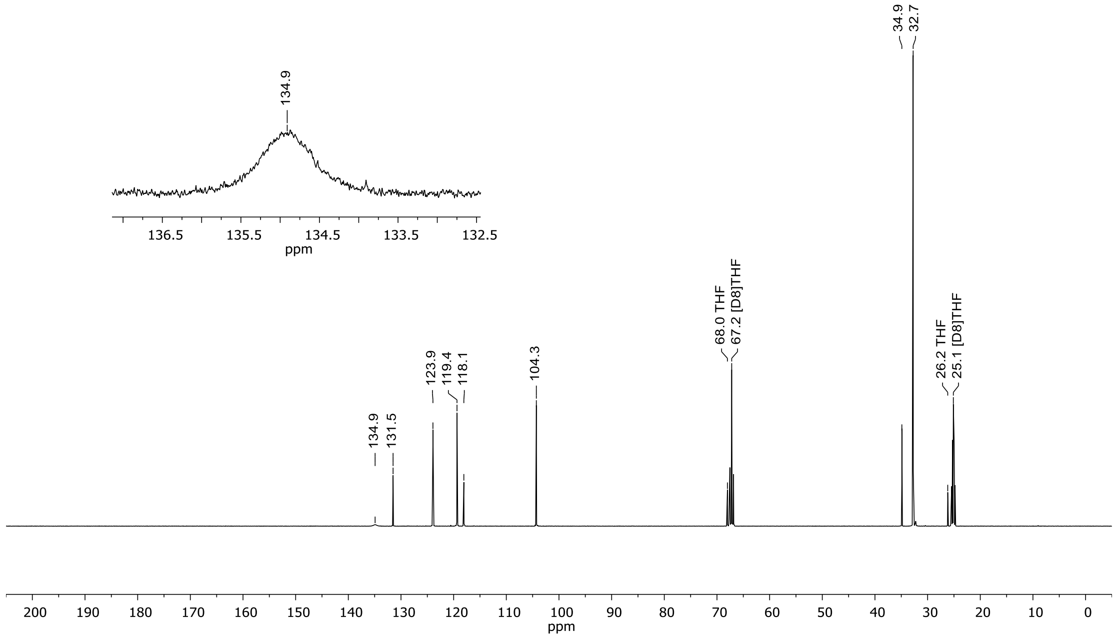

Figure S12: $^{13}C\{^{1}H\}$ NMR spectrum of Na_2[**1**] (125.8 MHz, [D_8]THF).

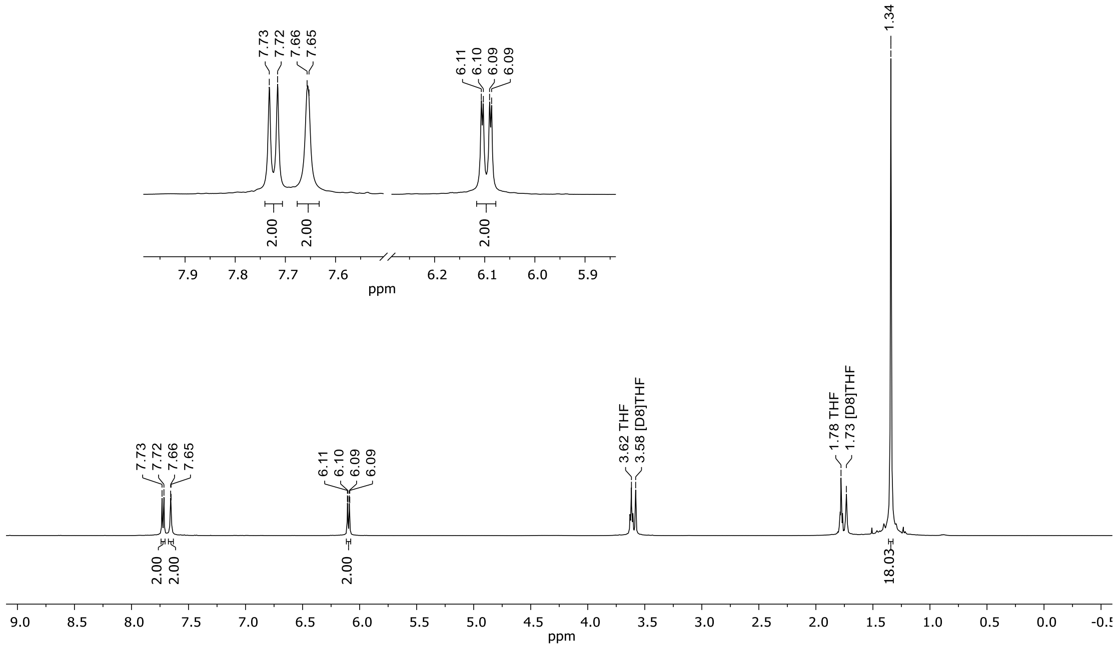

Figure S13: ^{1}H NMR spectrum of K_2[**1**] (500.2 MHz, [D_8]THF).

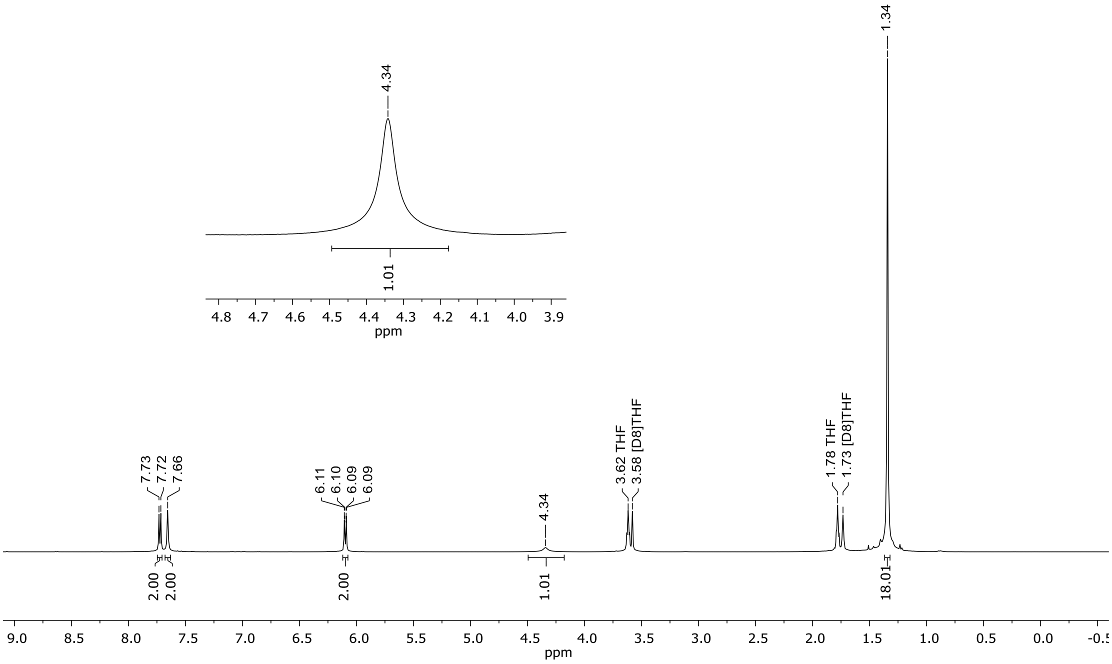

Figure S14: $^{1}H\{^{11}B\}$ NMR spectrum of K_2[**1**] (500.2 MHz, [D_8]THF).

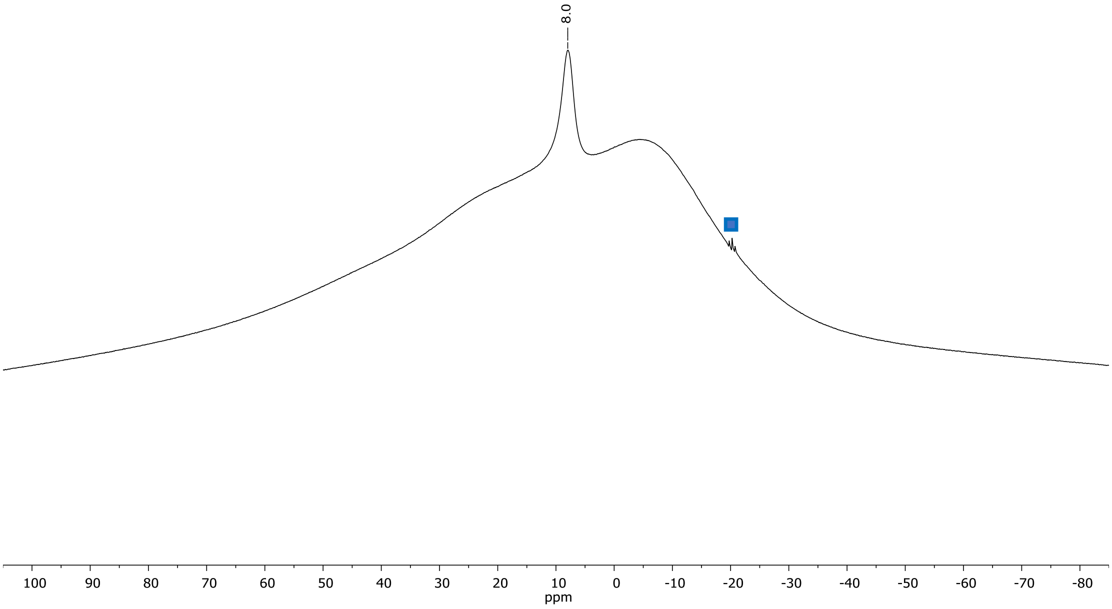

Figure S15: ^{11}B NMR spectrum of K_2[**1**] (160.5 MHz, [D_8]THF). Observed minor component: K[**1H**] (■, triplet).[S4]

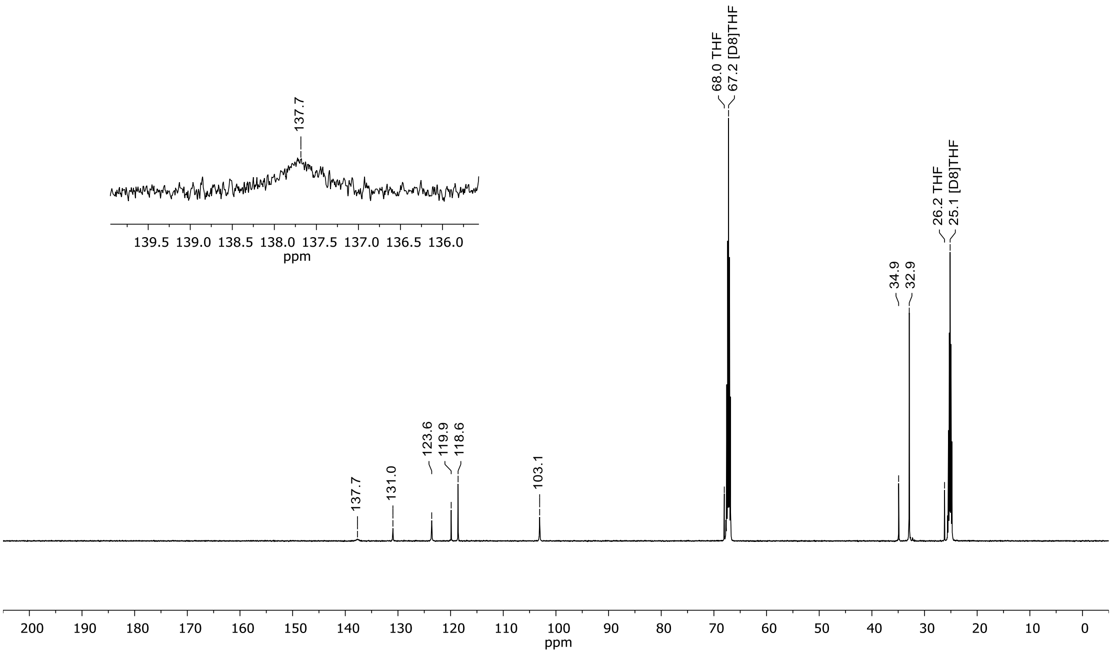

Figure S16: $^{13}C\{^{1}H\}$ NMR spectrum of K_2[**1**] (125.8 MHz, $[D_8]$THF).

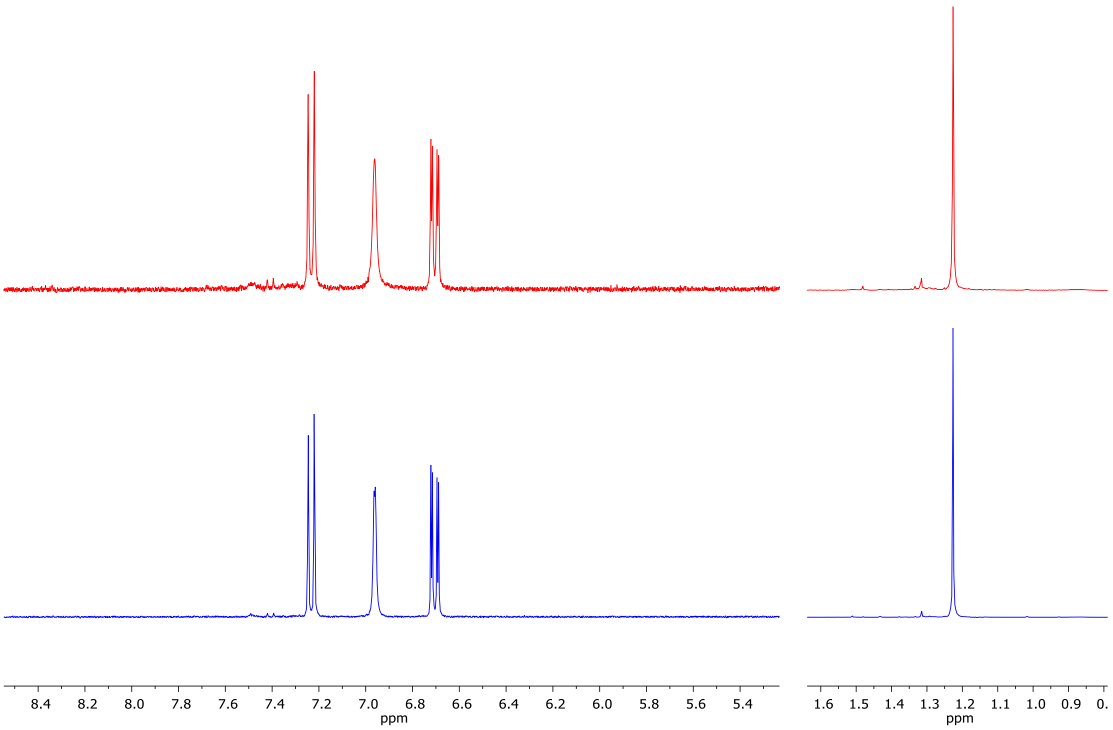

Figure S17: Characteristic sections of the ^{1}H NMR spectra (300.0 MHz, $[D_8]$THF) of the crude reaction mixture of Li_2[**2**] (red, top) and the pure product after recrystallization (blue, bottom). *Note:* The intensities of the aliphatic *vs*. aromatic signals are scaled differently.

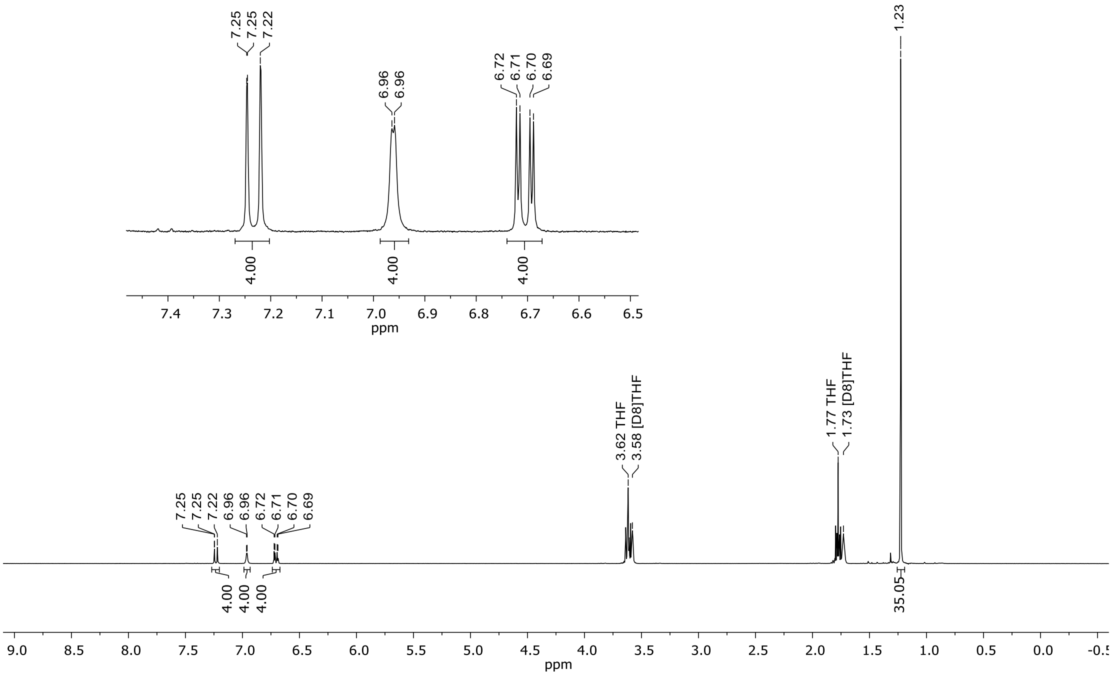

Figure S18: ^{1}H NMR spectrum of purified Li_2[**2**] (300.0 MHz, [D_8]THF).

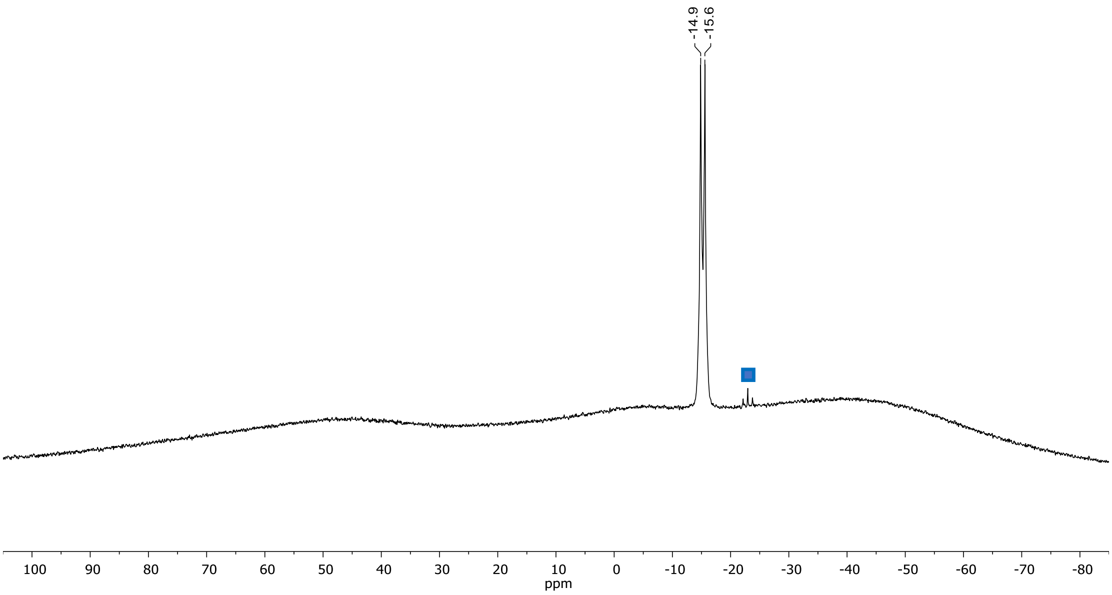

Figure S19: ^{11}B NMR spectrum of purified Li_2[**2**] (96.3 MHz, [D_8]THF). Observed minor component: Li[**1H**] (■, triplet).

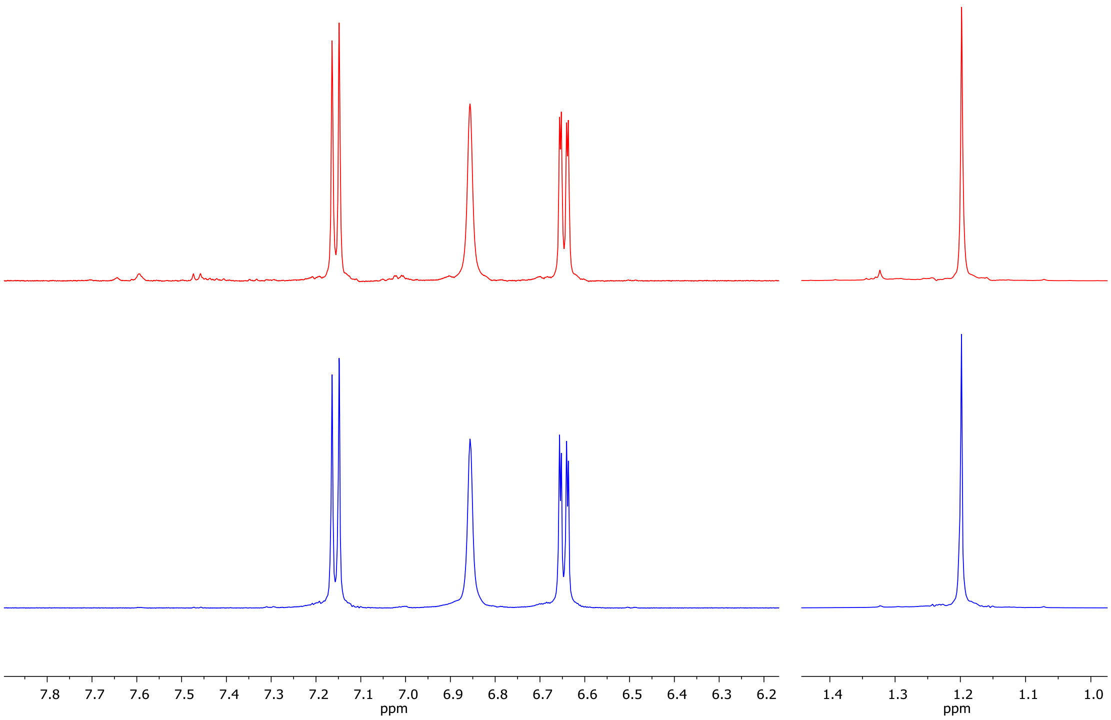

Figure S20: Characteristic sections of the ^{1}H NMR spectra (500.2 MHz, [D$_8$]THF) of the crude reaction mixture of Na$_2$[**2**] (red, top) and the product after recrystallization (blue, bottom). *Note:* The intensities of the aliphatic *vs*. aromatic signals are scaled differently.

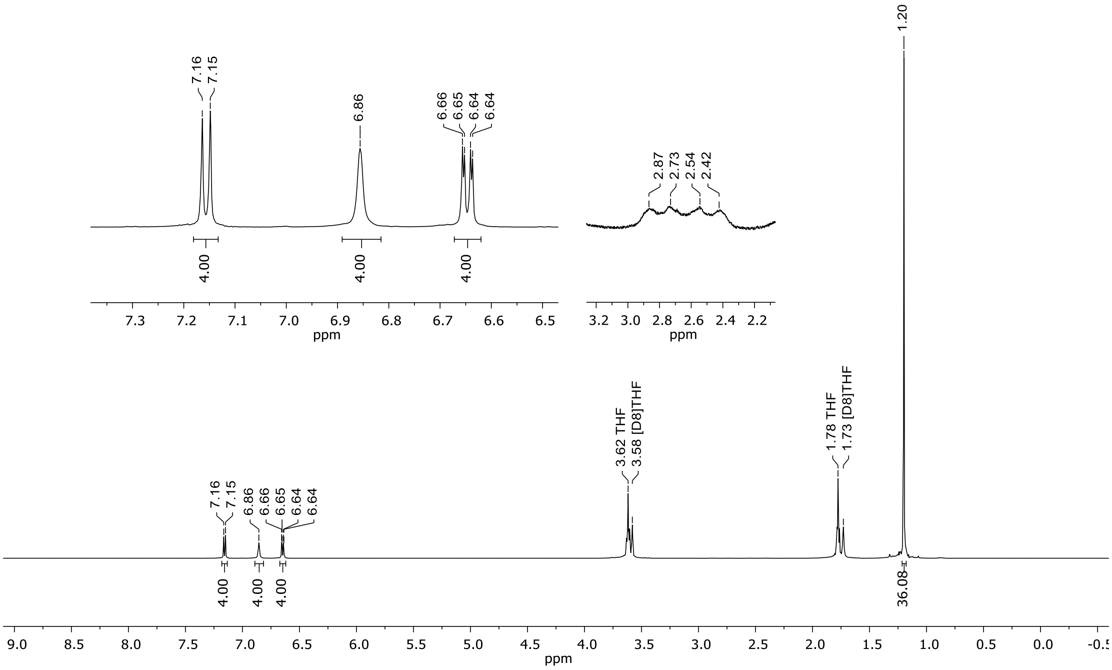

Figure S21: ^{1}H NMR spectrum of purified Na$_2$[**2**] (500.2 MHz, [D$_8$]THF).

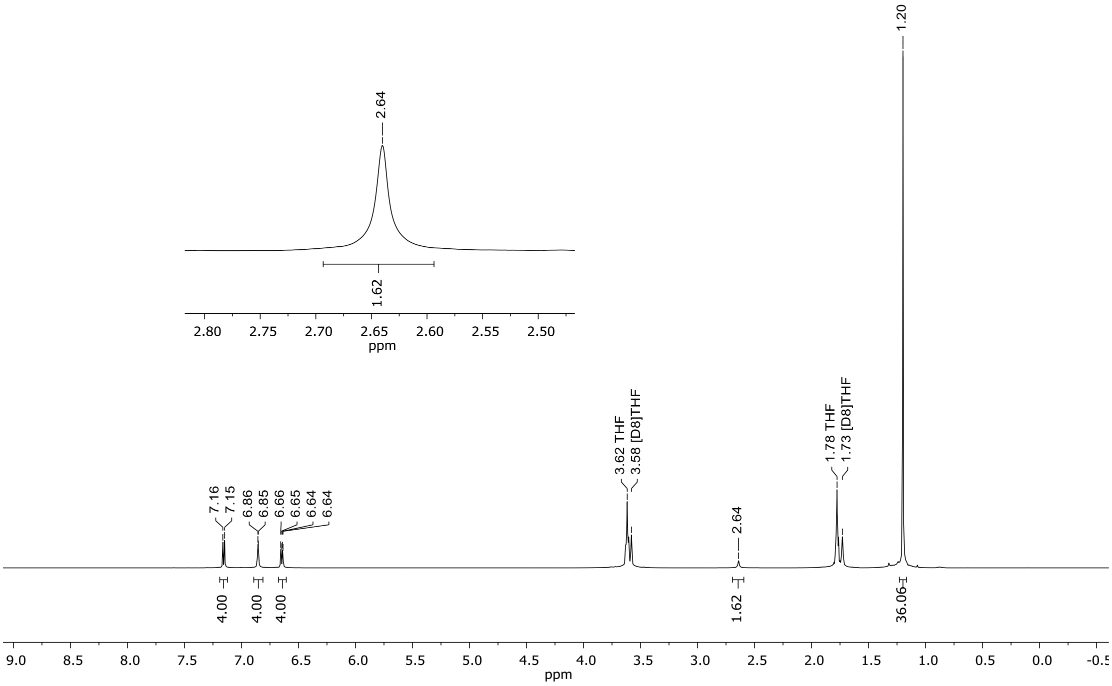

Figure S22: $^{1}H\{^{11}B\}$ NMR spectrum of purified Na_2[**2**] (500.2 MHz, $[D_8]$THF).

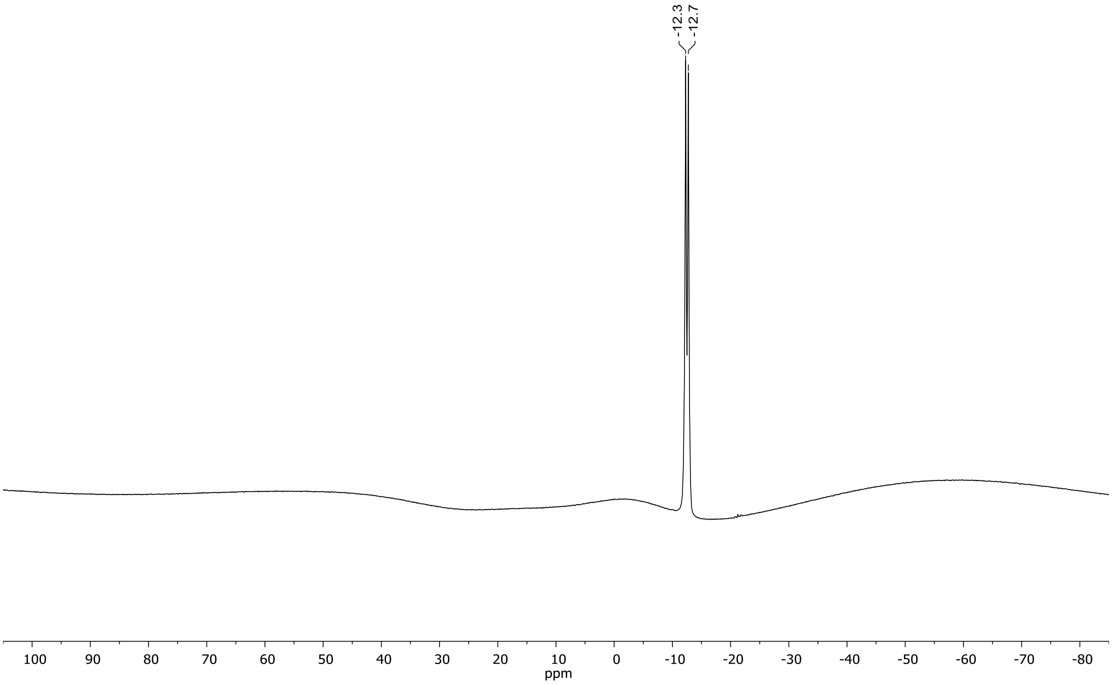

Figure S23: ^{11}B NMR spectrum of purified Na_2[**2**] (160.5 MHz, $[D_8]$THF).

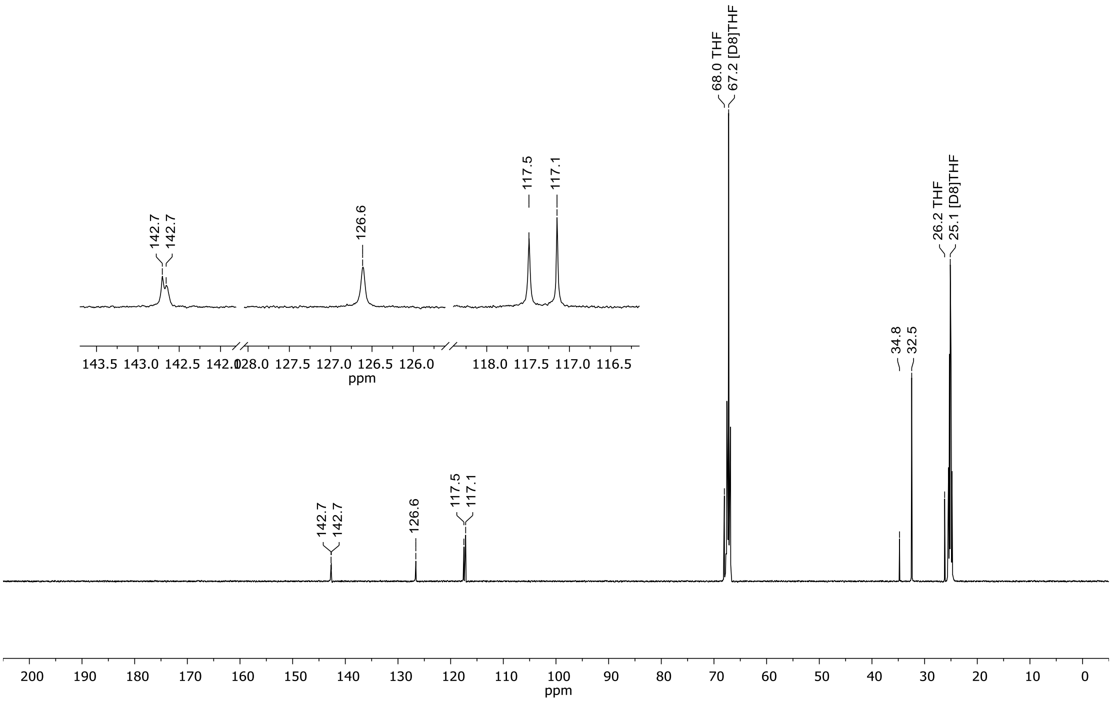

Figure S24: $^{13}C\{^{1}H\}$ NMR spectrum of purified Na_2[**2**] (125.8 MHz, [D_8]THF).

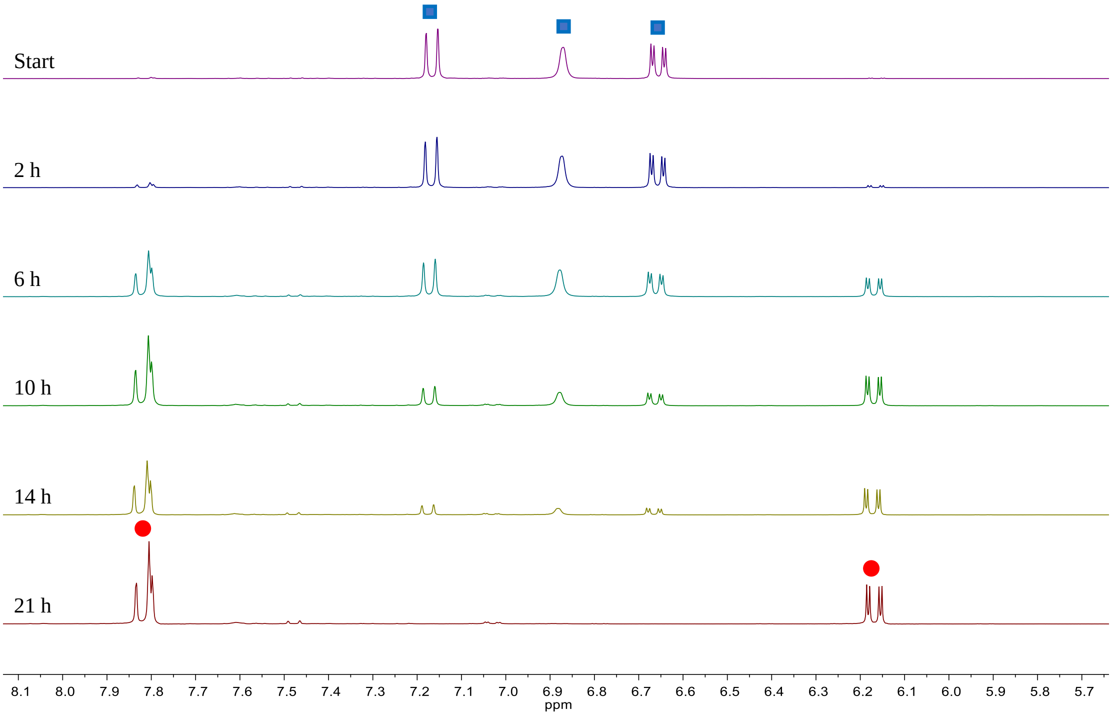

Figure S25: Aromatic regions of the ^{1}H NMR spectra (300.0 MHz, [D_8]THF) corresponding to different stages of the stepwise reduction of Na_2[**2**] with sodium metal. Marked components: Na_2[**2**] (🟦), Na_2[**1**] (●).

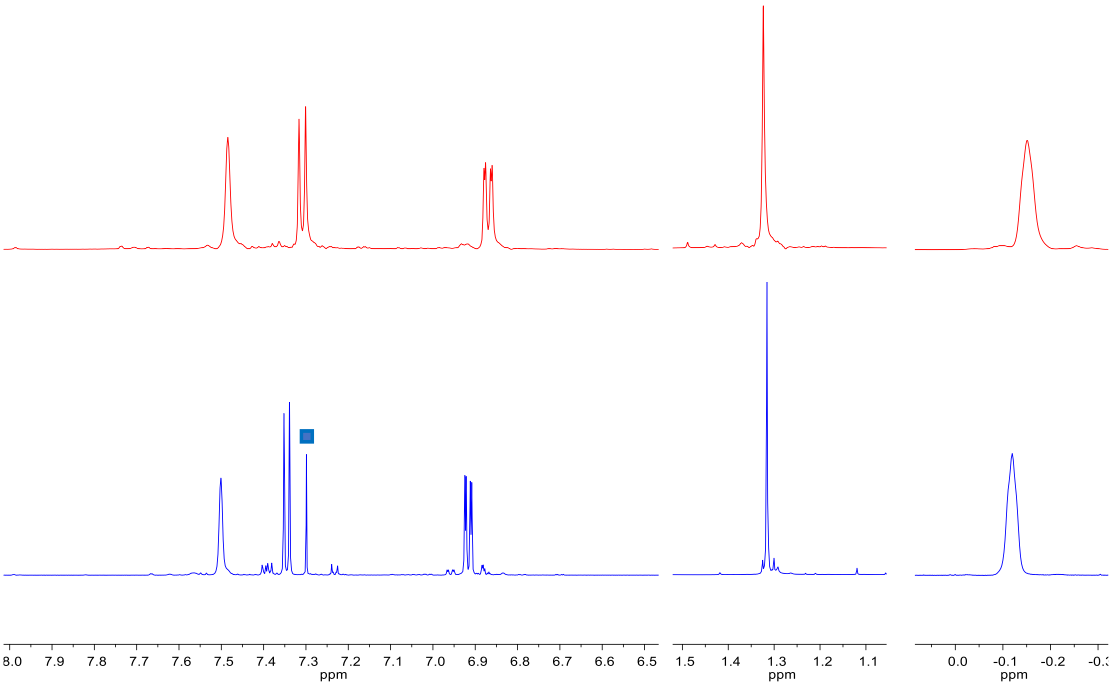

Figure S26: Characteristic sections of the ^{1}H NMR spectra of crude Li[**1Me**], synthesized from Li_2[**1**] and 1 equiv of MeCl (500.2 MHz, [D_8]THF; red, top), or from **4** and $LiAlH_4$ (600.3 MHz, [D_8]THF; blue, bottom). *Note:* The intensities of signals belonging to different sections are scaled differently. The resonance of residual C_6H_6 (■) originates from the extraction process.

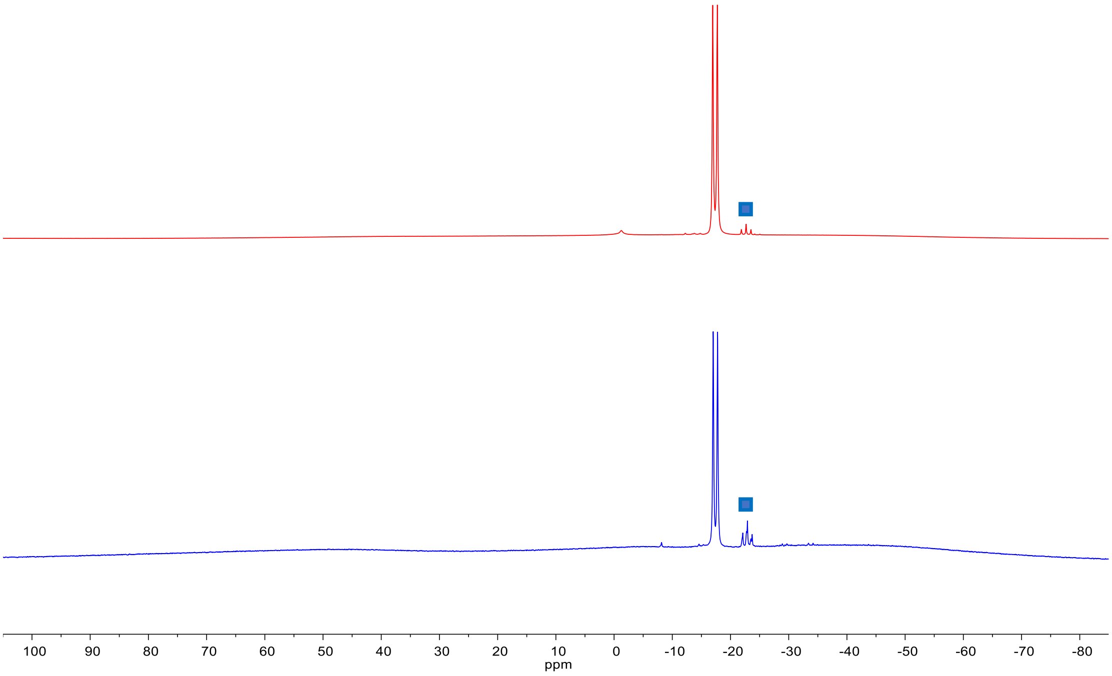

Figure S27: ^{11}B NMR spectra (96.3 MHz, [D_8]THF) of crude Li[**1Me**], synthesized from Li_2[**1**] and 1 equiv of MeCl (red, top), or from **4** and $LiAlH_4$ (blue, bottom). Observed minor component: Li[**1H**] (■, triplet).

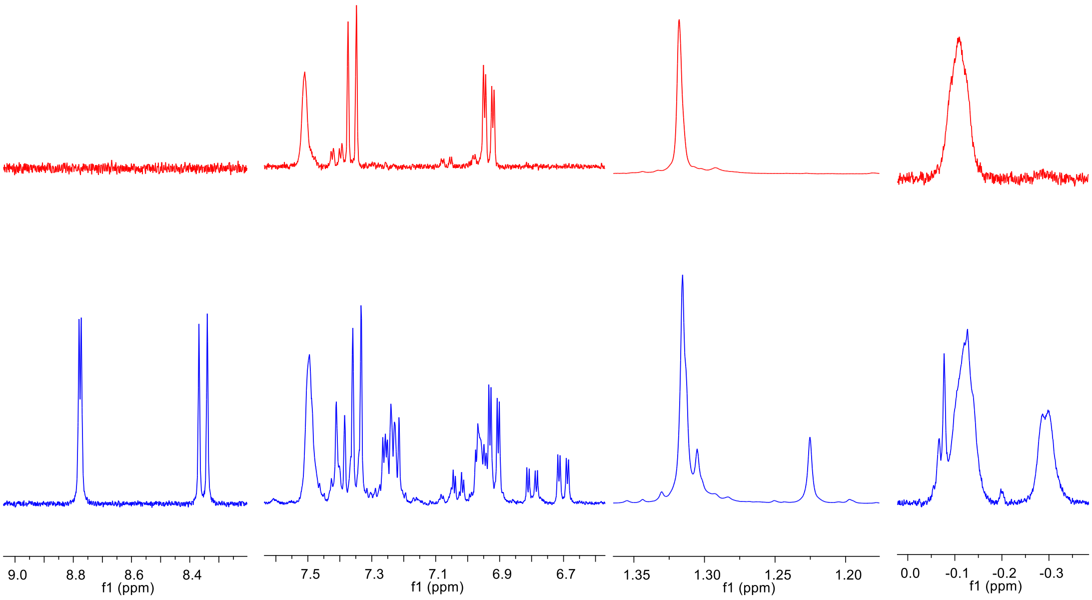

Figure S28: Characteristic sections of the ^{1}H NMR spectra (300.0 MHz, [D$_8$]THF) of crude Li[**1Me**], synthesized from Li$_2$[**1**] and 1 equiv of MeCl (red, top), or from Li$_2$[**1**] and 1 equiv of MeI (blue, bottom; major side products are Li[**1H**], Li$_2$[**2**], and Li[**3H**]). *Note:* The intensities of signals belonging to different sections are scaled differently.

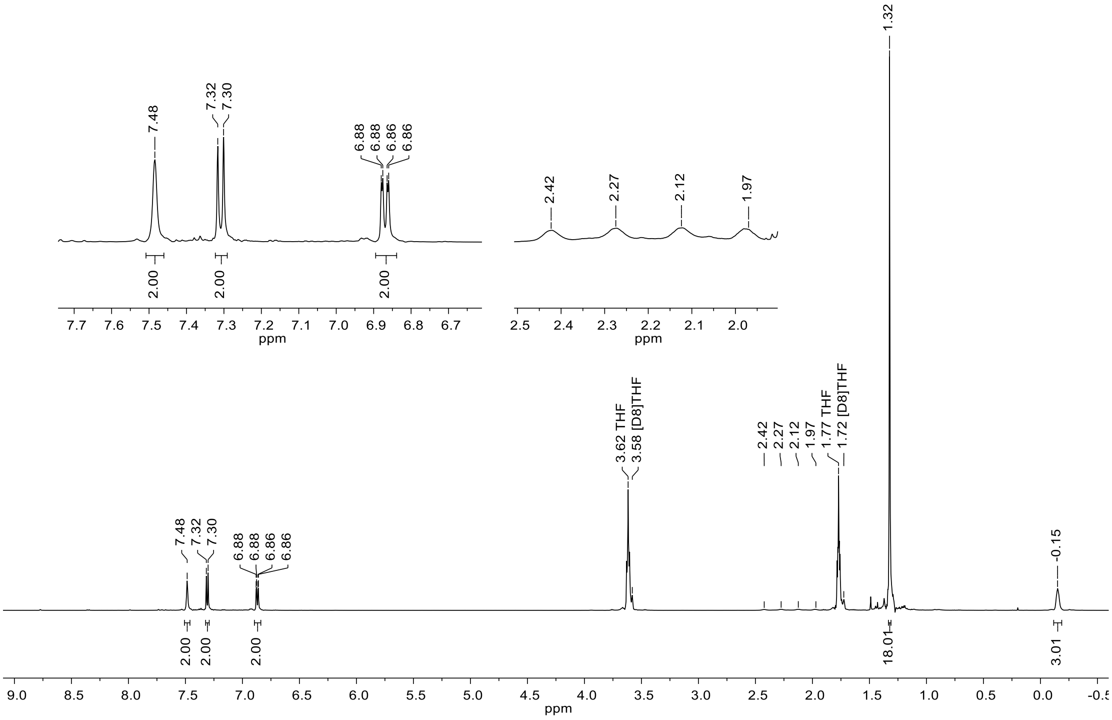

Figure S29: ^{1}H NMR spectrum of Li[**1Me**] (500.2 MHz, [D$_8$]THF).

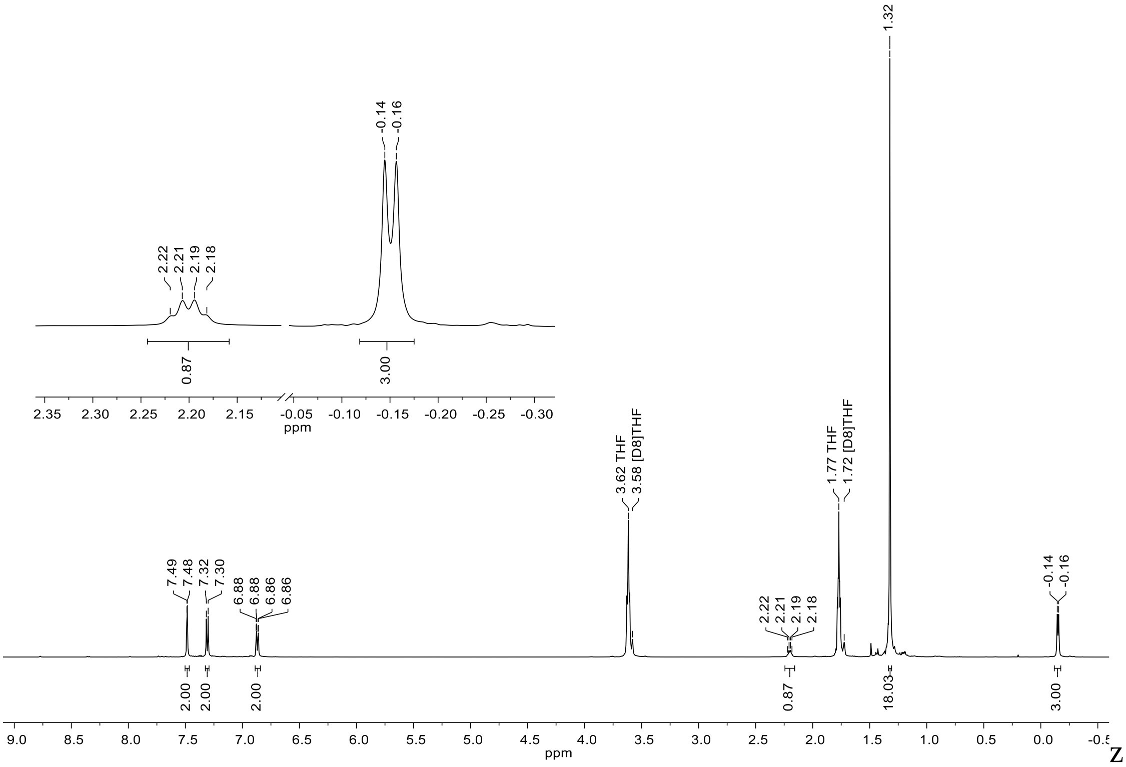

Figure S30: $^{1}H\{^{11}B\}$ NMR spectrum of Li[**1Me**] (500.2 MHz, [D$_8$]THF).

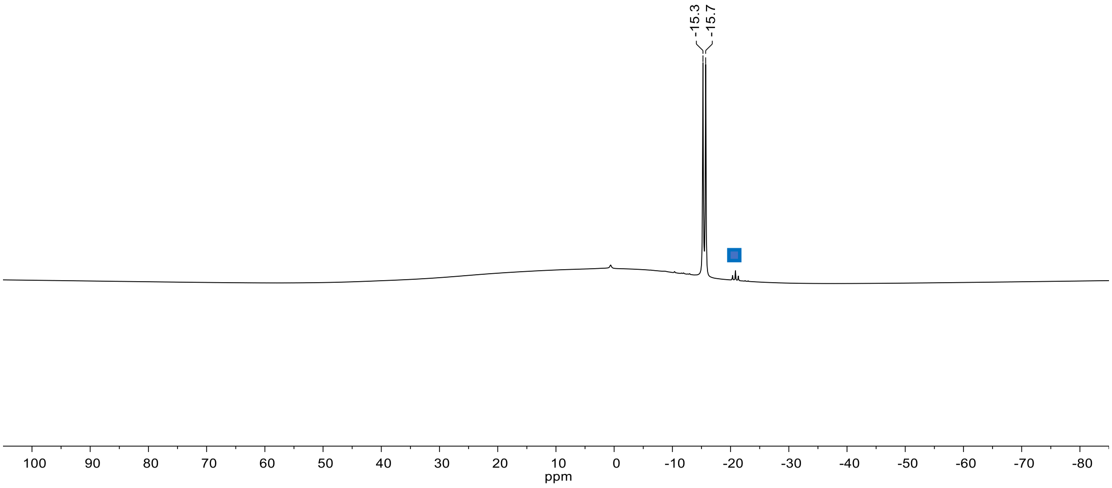

Figure S31: ^{11}B NMR spectrum of Li[**1Me**] (160.5 MHz, [D$_8$]THF). Observed minor component: Li[**1H**] (■, triplet).

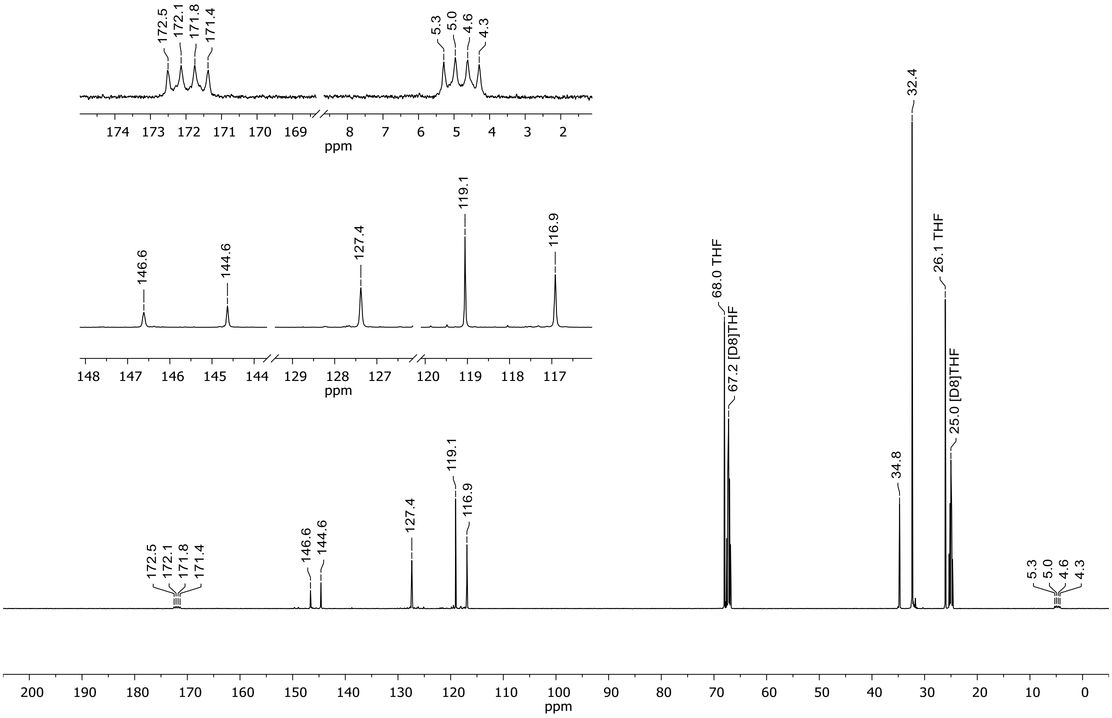

Figure S32: $^{13}C\{^{1}H\}$ NMR spectrum of Li[**1Me**] (125.8 MHz, [D$_8$]THF).

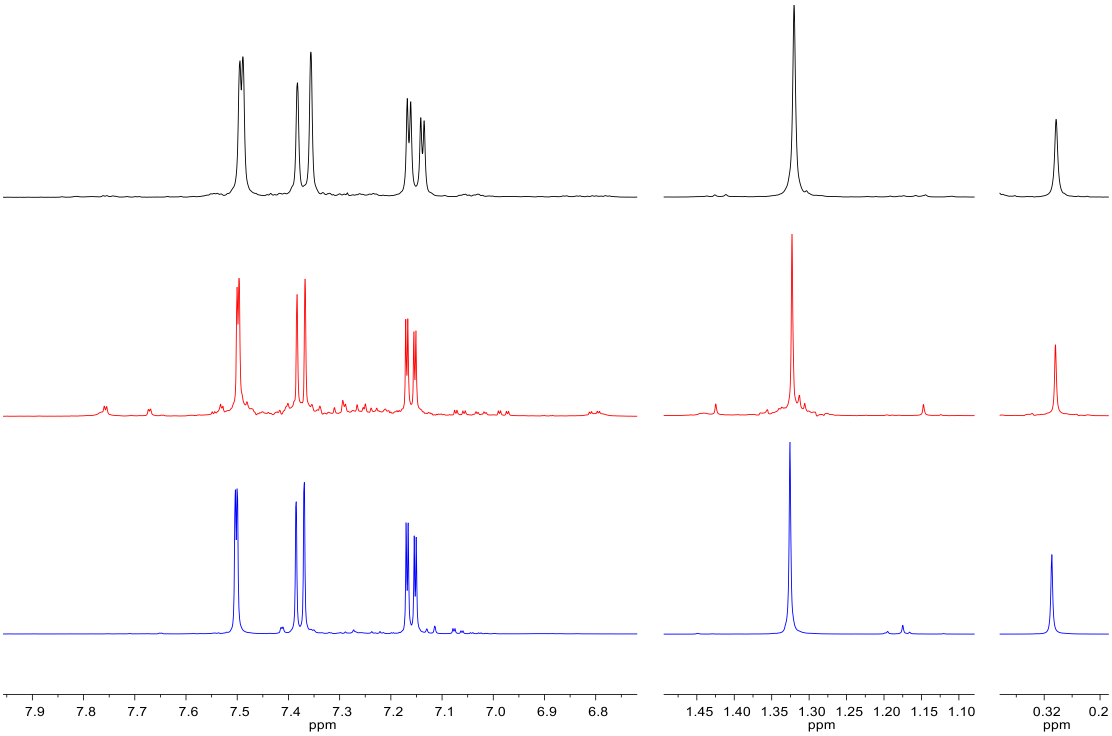

Figure S33: Characteristic sections of the ^{1}H NMR spectra of **4**, obtained from Li$_2$[**1**], 1 equiv MeCl, and TMSCl (*Method A*; 300.0 MHz, [D$_8$]THF; black, top), or from Li$_2$[**1**] and excess MeCl (*Method B*; 500.2 MHz, [D$_8$]THF; red, middle), or *via* the published synthesis of **4** (500.2 MHz, [D$_8$]THF; blue, bottom).[S2] *Note:* The intensities of signals belonging to different sections are scaled differently.

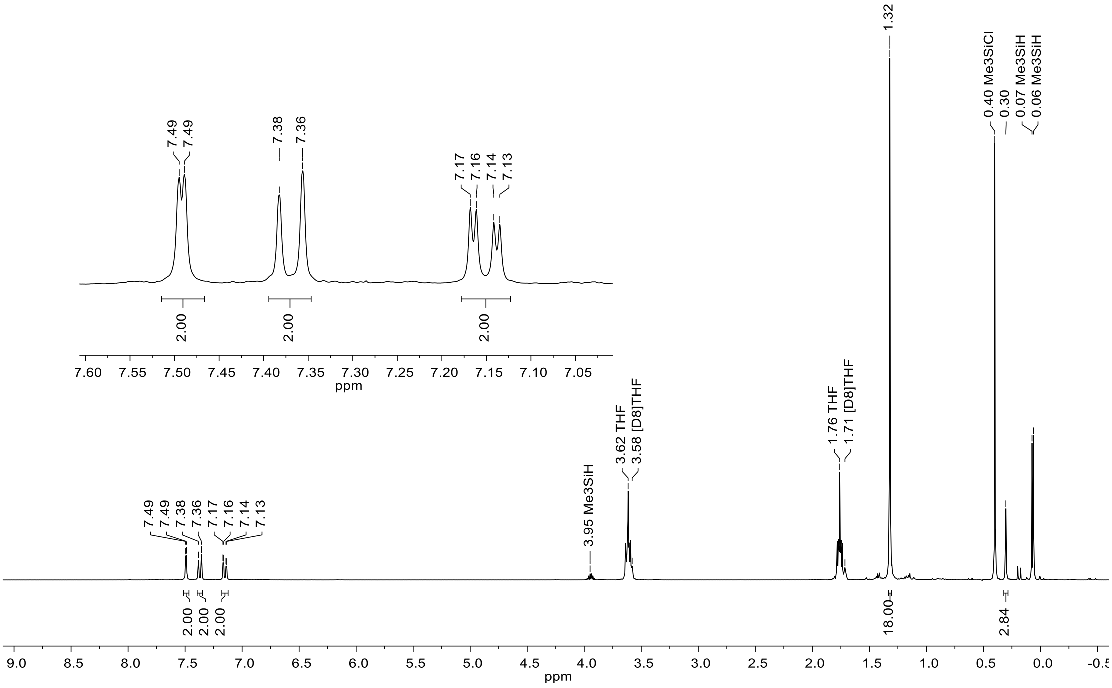

Figure S34: ^{1}H NMR spectrum of **4**; crude reaction mixture obtained *via* 'Method A' (300.0 MHz, [D$_8$]THF).

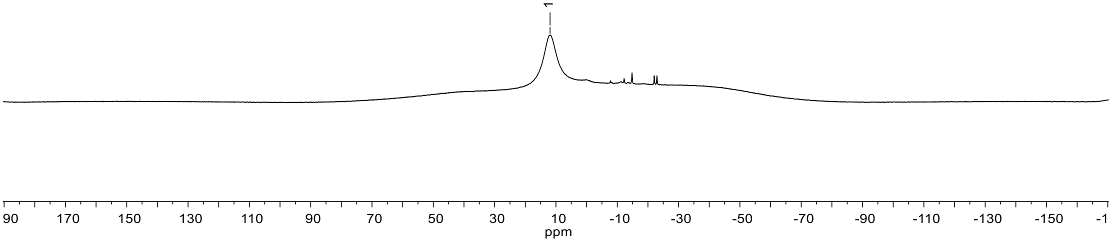

Figure S35: ^{11}B NMR spectrum of **4**; crude reaction mixture obtained *via* 'Method A' (96.3 MHz, [D$_8$]THF).

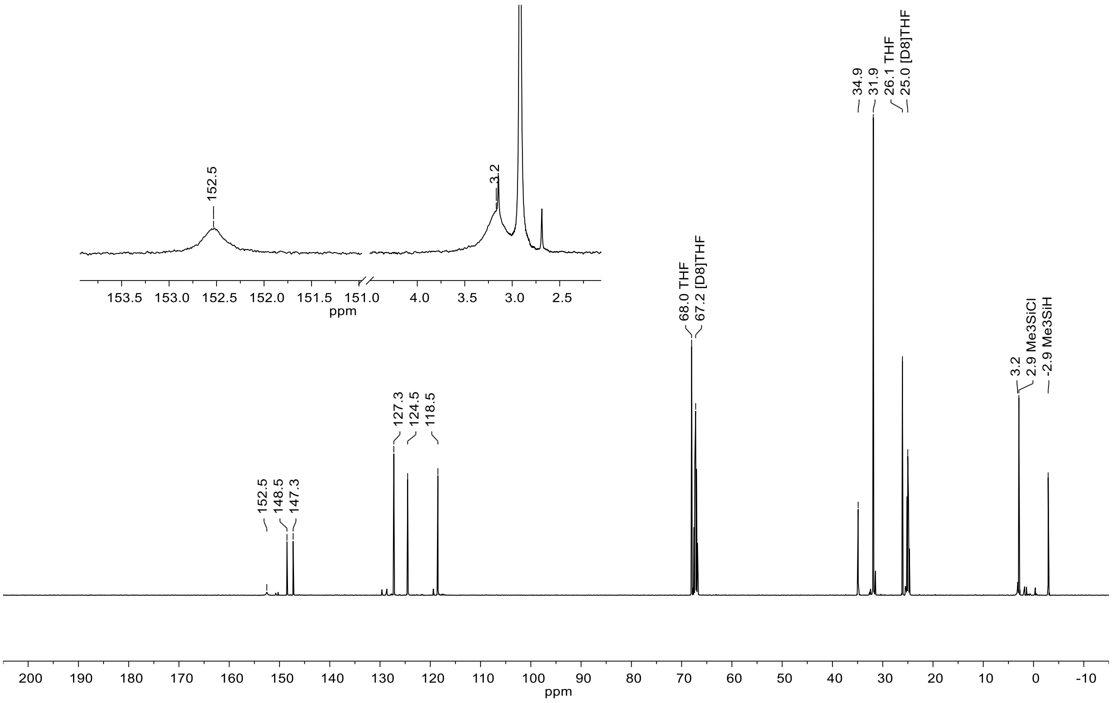

Figure S36: ^{13}C NMR spectrum of **4**; crude reaction mixture obtained *via* ‘Method A’ (125.8 MHz, [D$_8$]THF).

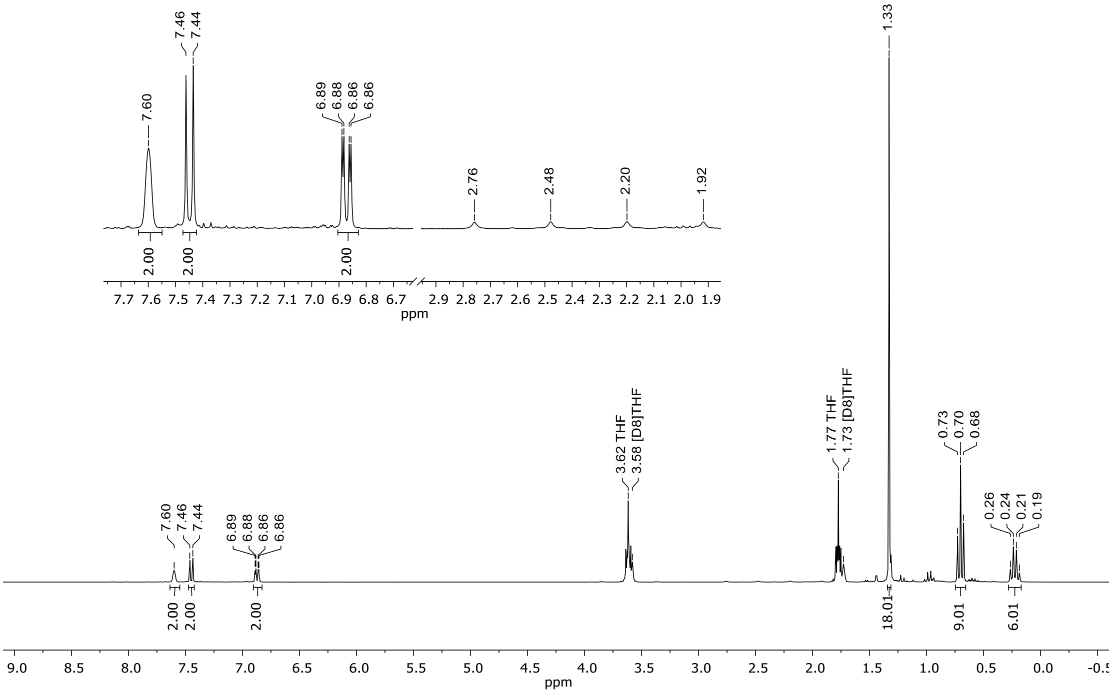

Figure S37: ^{1}H NMR spectrum of Li[**1SiEt$_3$**] (300.0 MHz, [D$_8$]THF).

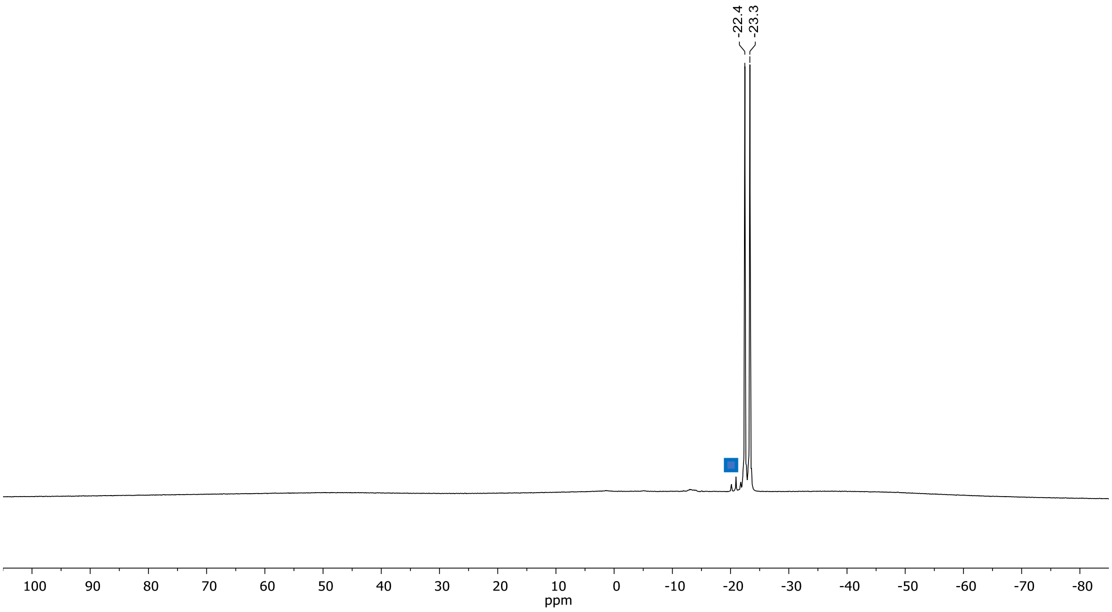

Figure S38: ^{11}B NMR spectrum of Li[**1SiEt$_3$**] (96.3 MHz, [D$_8$]THF). Observed minor component: Li[**1H**] (■, triplet).

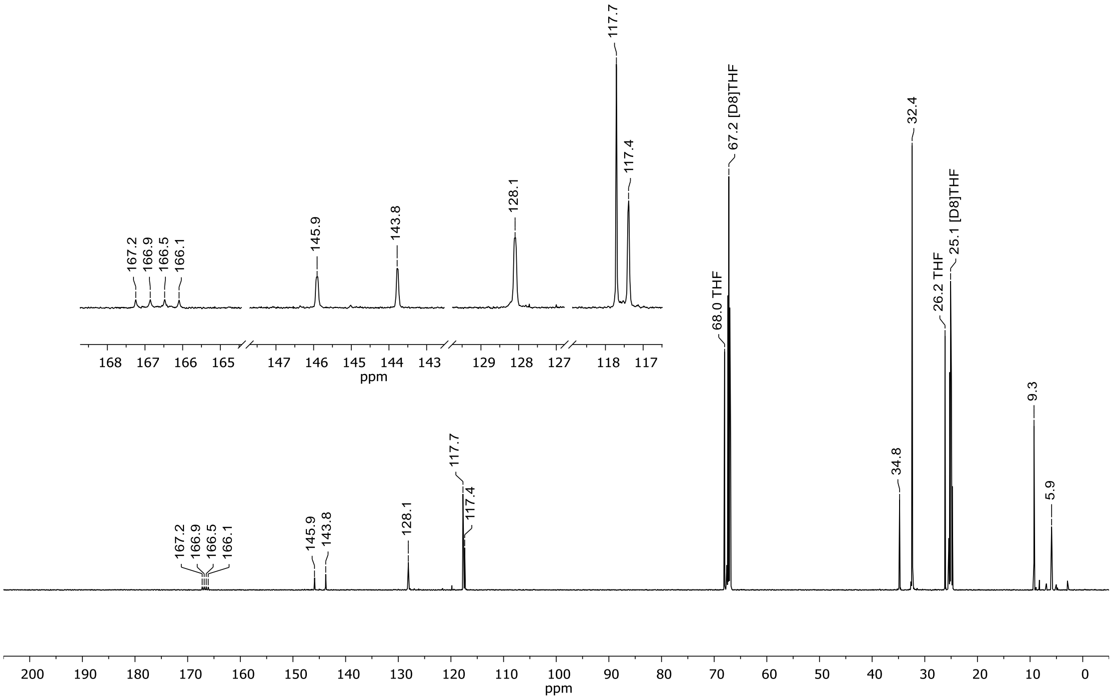

Figure S39: ^{13}C NMR spectrum of Li[**1SiEt$_3$**] (125.8 MHz, [D$_8$]THF).

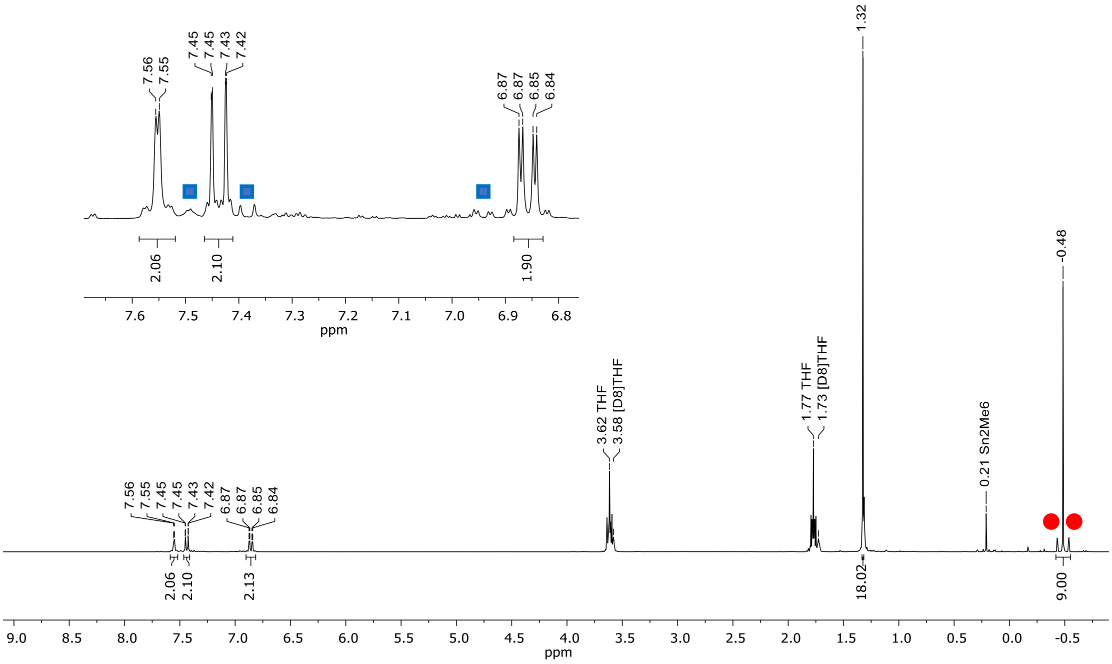

Figure S40: ^{1}H NMR spectrum of Li[**1SnMe$_3$**]; crude reaction mixture (500.2 MHz, [D$_8$]THF). Observed minor component: Li[**1H**] (■). The $^{117/119}$Sn satellites of the BSn(CH_3) resonance are marked with (●).

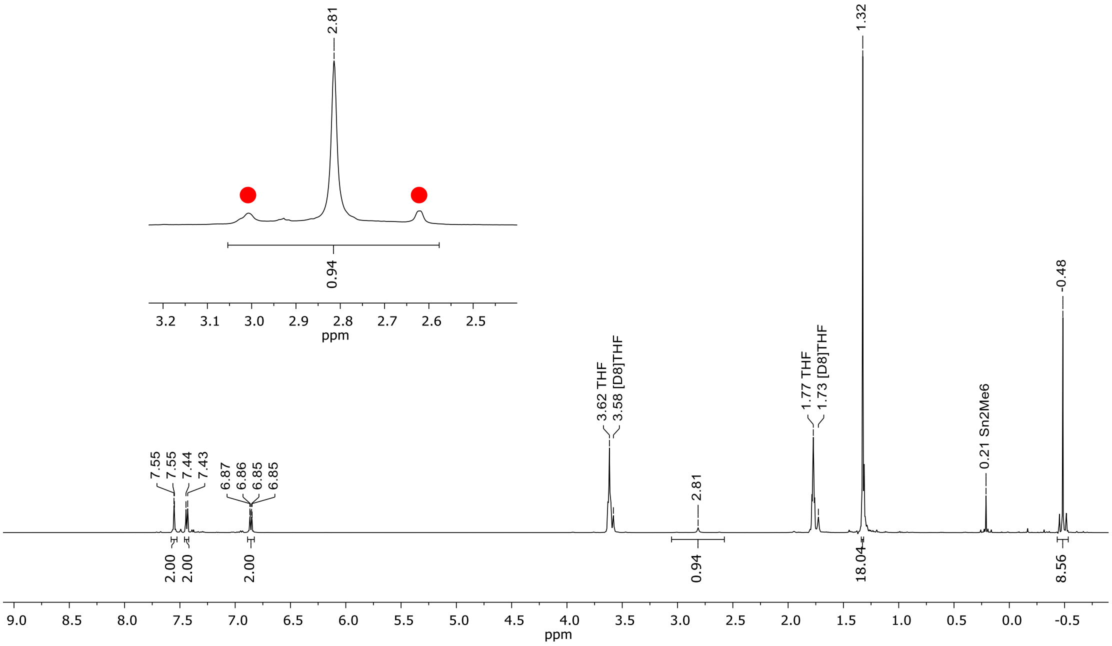

Figure S41: ^{1}H{^{11}B} NMR spectrum of Li[**1SnMe$_3$**] (500.2 MHz, [D$_8$]THF). The $^{117/119}$Sn satellites of the HBSn resonance are marked with (●).

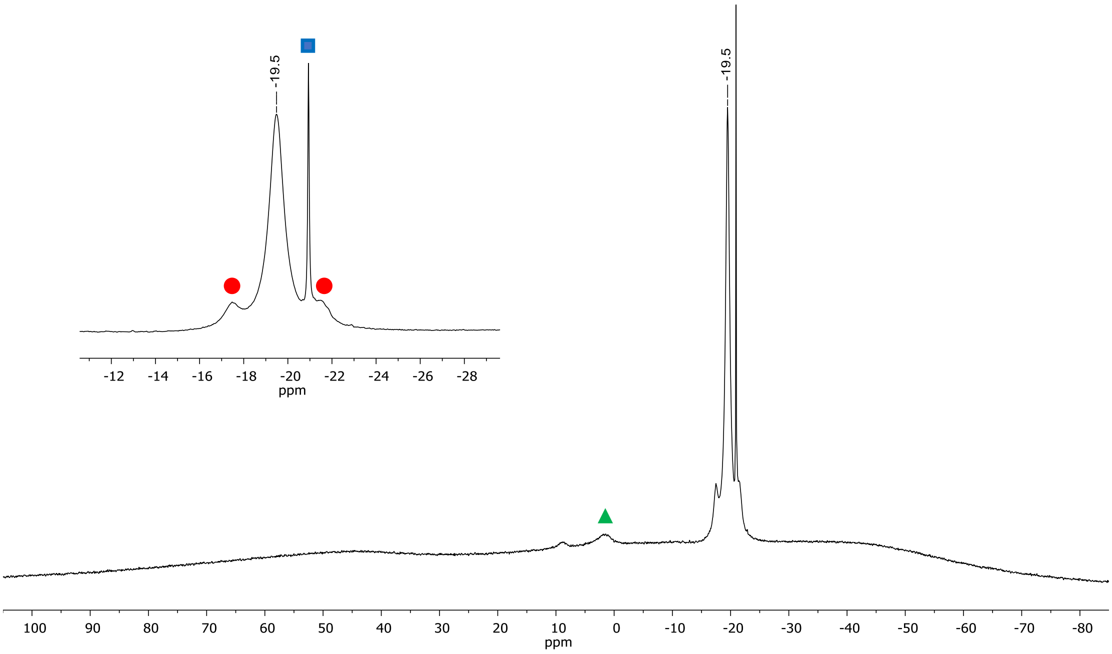

Figure S42: $^{11}B\{^1H\}$ NMR spectrum of Li[**1SnMe**$_3$] (160.5 MHz, [D$_8$]THF). Observed minor components: Li[**1H**] (■, sharp singlet (due to proton decoupling)), Li$_2$[**1**] (▲). The $^{117/119}$Sn satellites of the *B*Sn resonance are marked with (●).

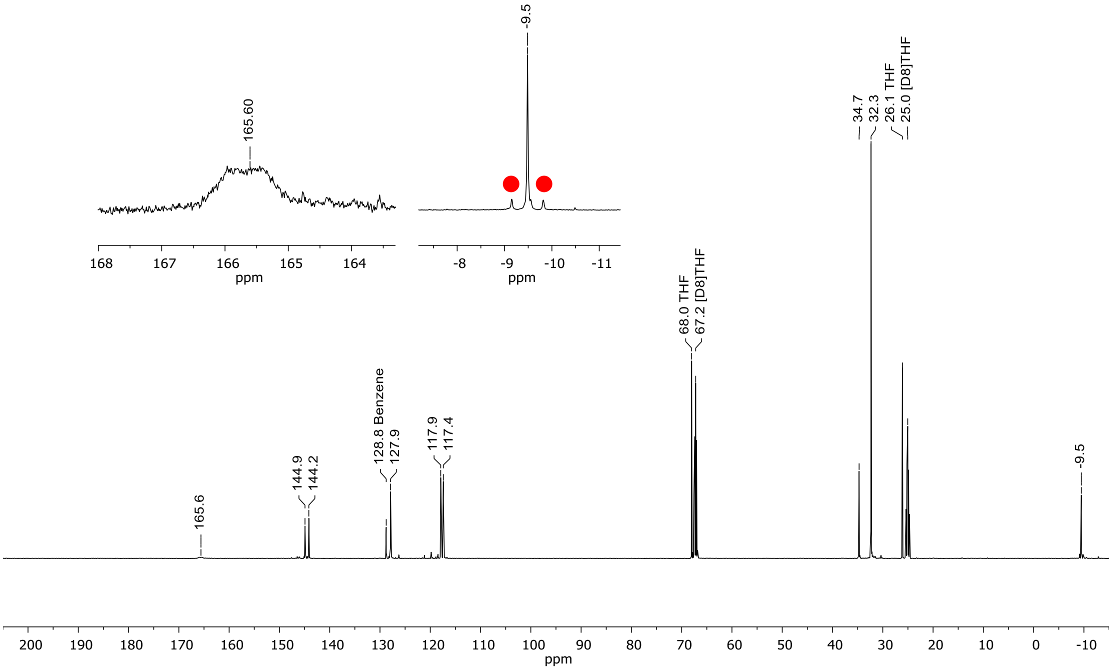

Figure S43: $^{13}C\{^1H\}$ NMR spectrum of Li[**1SnMe**$_3$] (125.8 MHz, [D$_8$]THF). The $^{117/119}$Sn satellites of the BSn(*C*H$_3$) resonance are marked with (●).

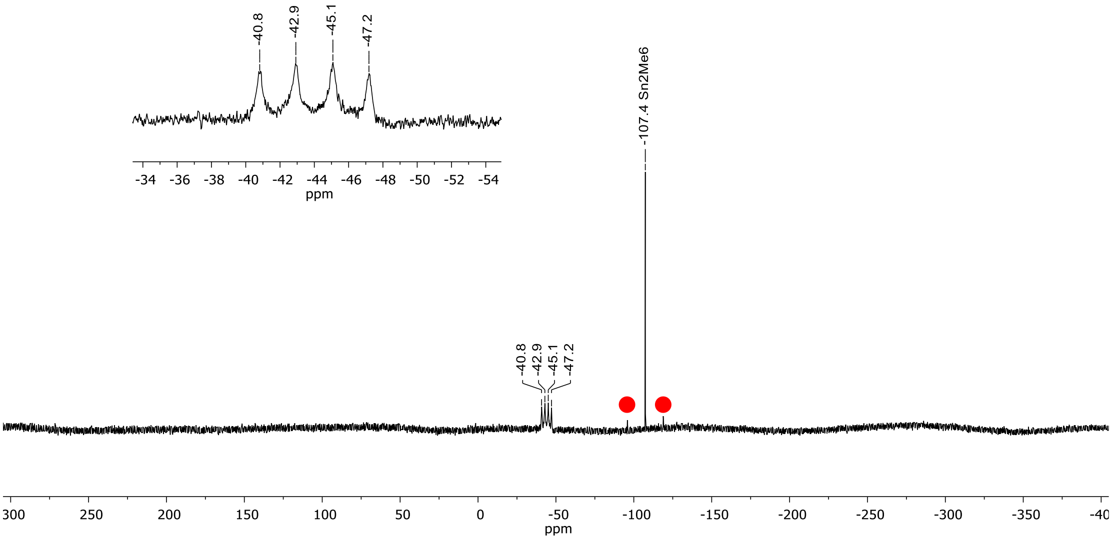

Figure S44: ^{119}Sn{^{1}H} NMR spectrum of Li[**1SnMe**$_3$] (186.5 MHz, [D$_8$]THF). The $^{117/119}$Sn satellites of the *Sn*$_2$Me$_6$ resonance are marked with (●).

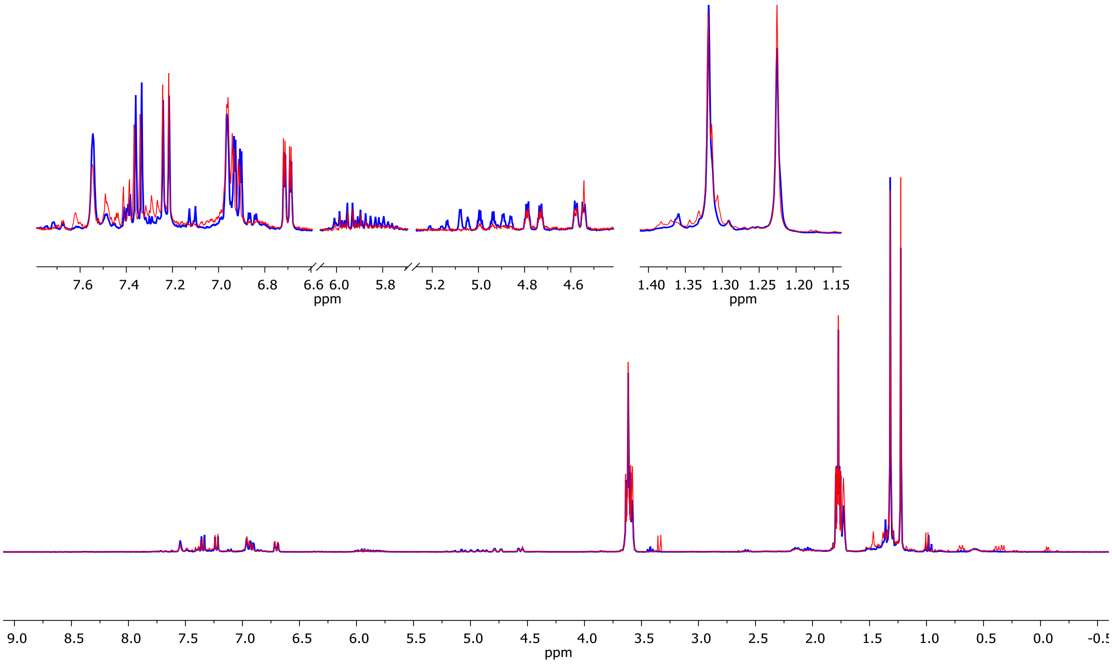

Figure S45: Superimposed ^{1}H NMR spectra (300.0 MHz, [D$_8$]THF) recorded on the reaction mixtures of Li$_2$[**1**] and (bromomethyl)cyclopropane (red) or 4-bromo-1-butene (blue).

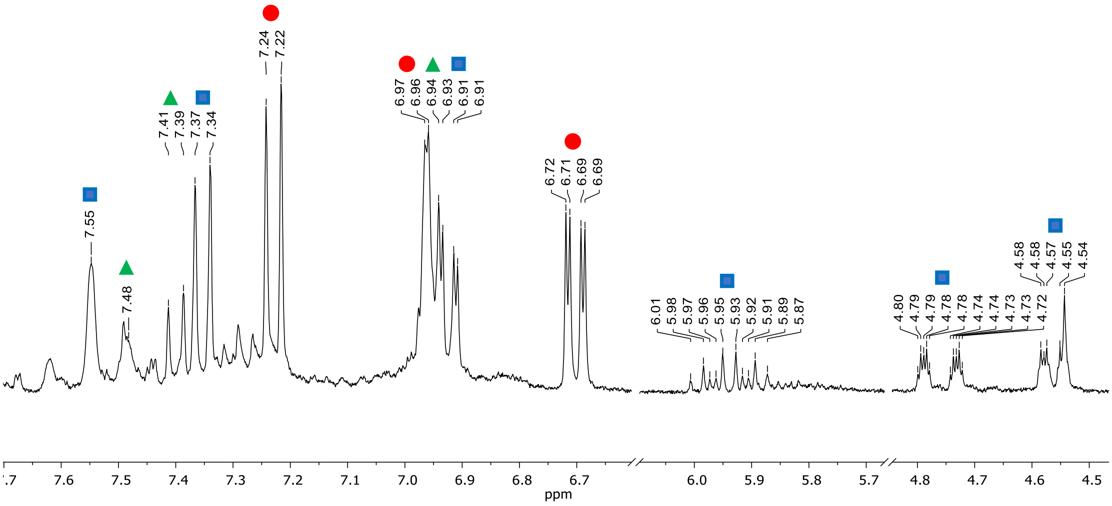

Figure S46: Aromatic and olefinic regions of the ^{1}H NMR spectrum (300.0 MHz, [D$_8$]THF) recorded on the reaction mixture of Li$_2$[**1**] and (bromomethyl)cyclopropane. Marked components: Li$_2$[**2**] (●), Li[**1C$_2$H$_4$CH=CH$_2$**] (■; BFlu = borafluorenyl), Li[**1H**] (▲).

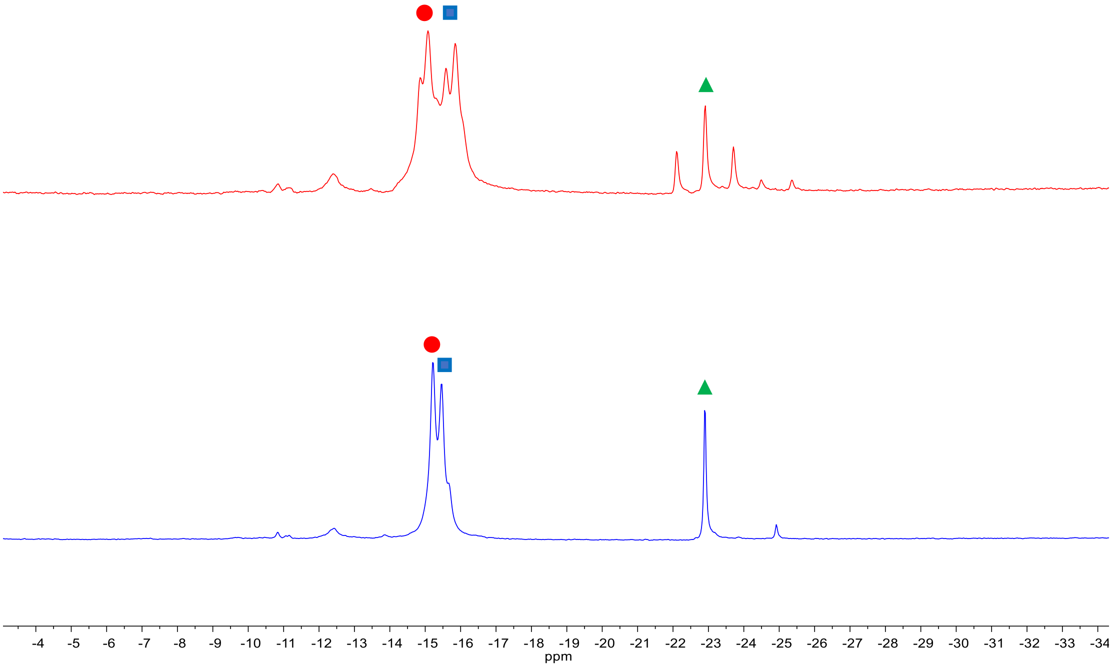

Figure S47: ^{11}B and ^{11}B{^{1}H} NMR spectrum (96.3 MHz, [D$_8$]THF) recorded on the reaction mixture of Li$_2$[**1**] and (bromomethyl)cyclopropane. Marked components: Li$_2$[**2**] (●), Li[**1C$_2$H$_4$CH=CH$_2$**](■; BFlu = borafluorenyl), Li[**1H**] (▲).

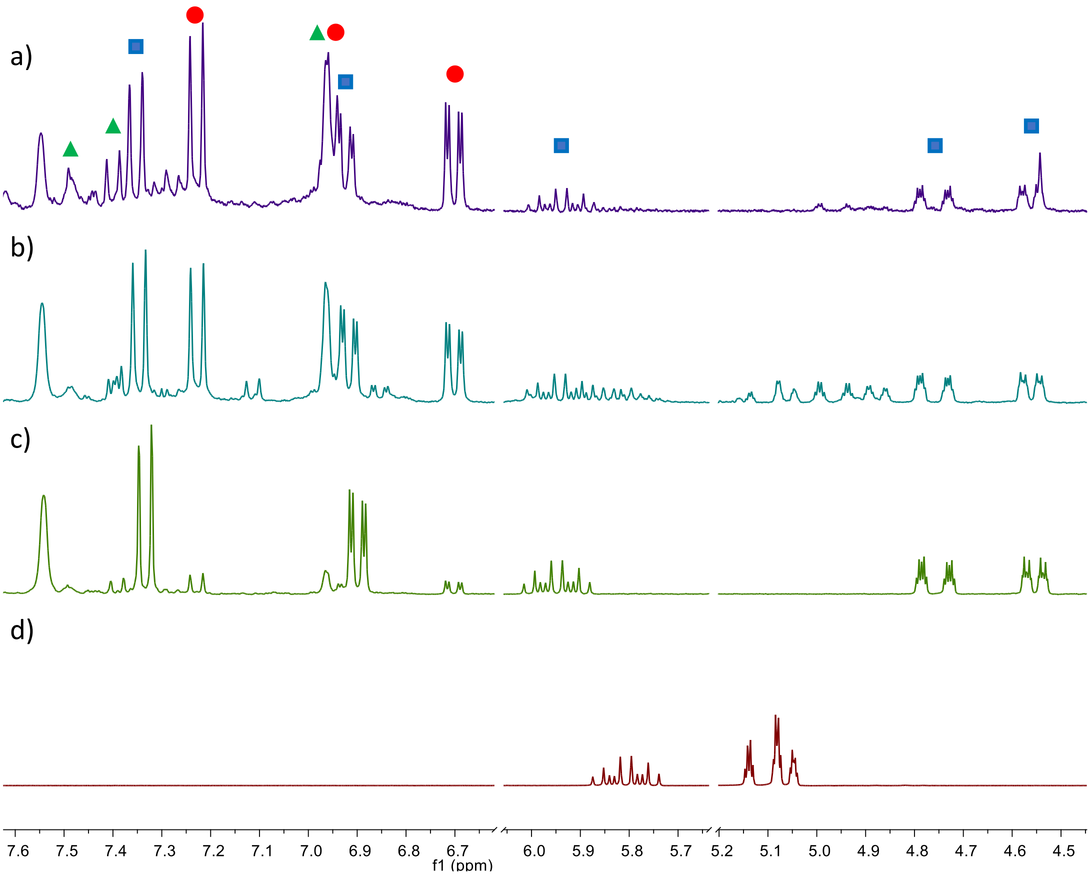

Figure S48: Aromatic and olefinic regions of the ^{1}H NMR spectrum (300.0 MHz, [D$_8$]THF) recorded on the reaction mixture of Li$_2$[**1**] and (bromomethyl)cyclopropane (a), or Li$_2$[**1**] and 4-bromo-1-butene (b), or an authentic sample of Li[**1C$_2$H$_4$CH=CH2**] from the reaction of Li$_2$[**1**] and 4-chloro-1-butene (c), or 4-bromo-1-butene (d). Marked components: Li$_2$[**2**] (●), Li[**1C$_2$H$_4$CH=CH2**] (■), Li[**1H**] (▲).

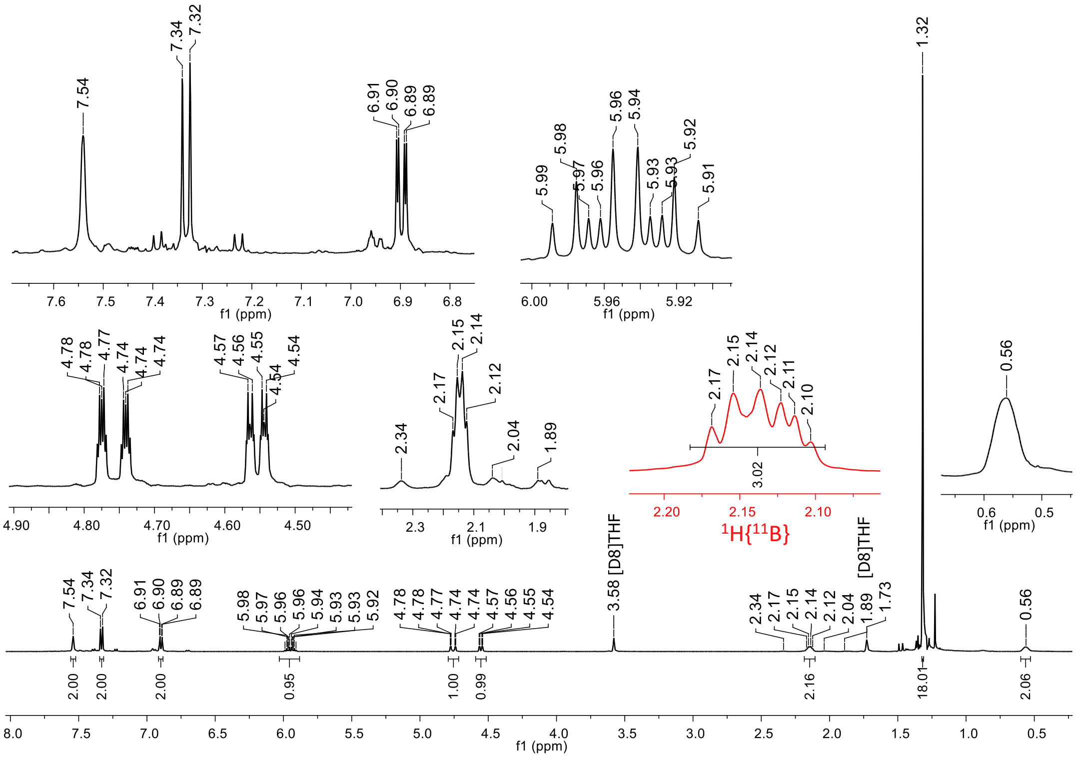

Figure S49: ^{1}H NMR spectrum and a section of the ^{1}H{^{11}B} NMR spectrum (red) of Li[**1C$_2$H$_4$CH=CH2**] (500.2 MHz, [D$_8$]THF).

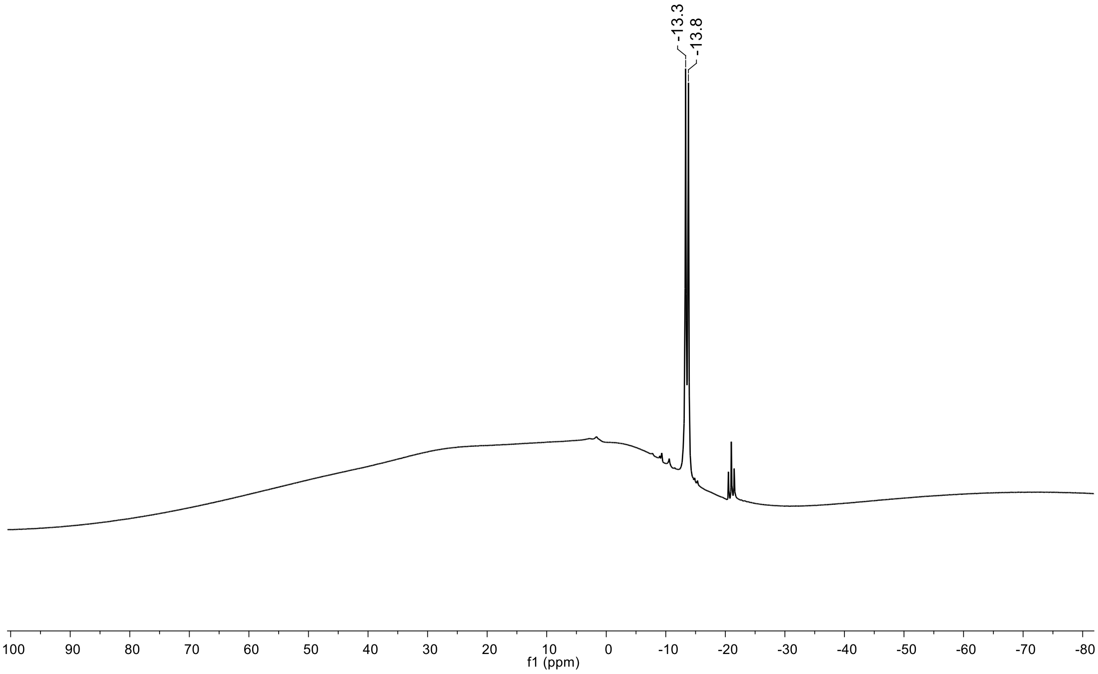

Figure S50: ^{11}B NMR spectrum of Li[**1C$_2$H$_4$CH=CH2**] (160.5 MHz, [D$_8$]THF).

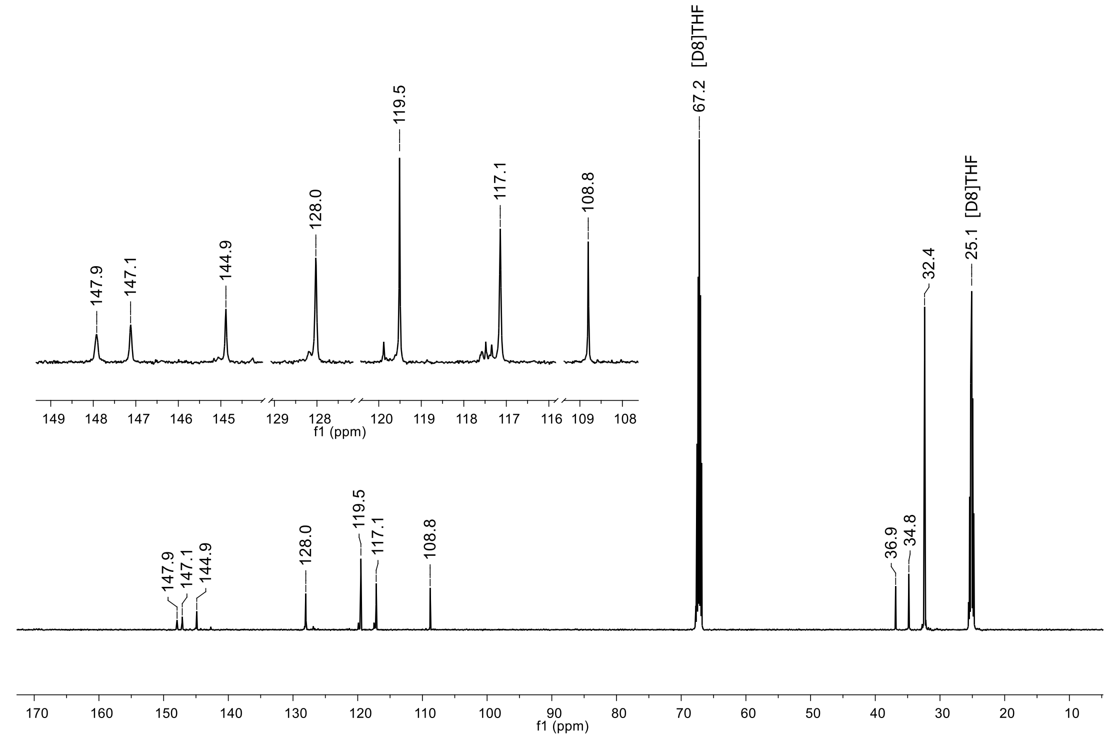

Figure S51: ^{13}C{^{1}H} NMR spectrum of Li[**1C$_2$H$_4$CH=CH2**] (125.8 MHz, [D$_8$]THF).

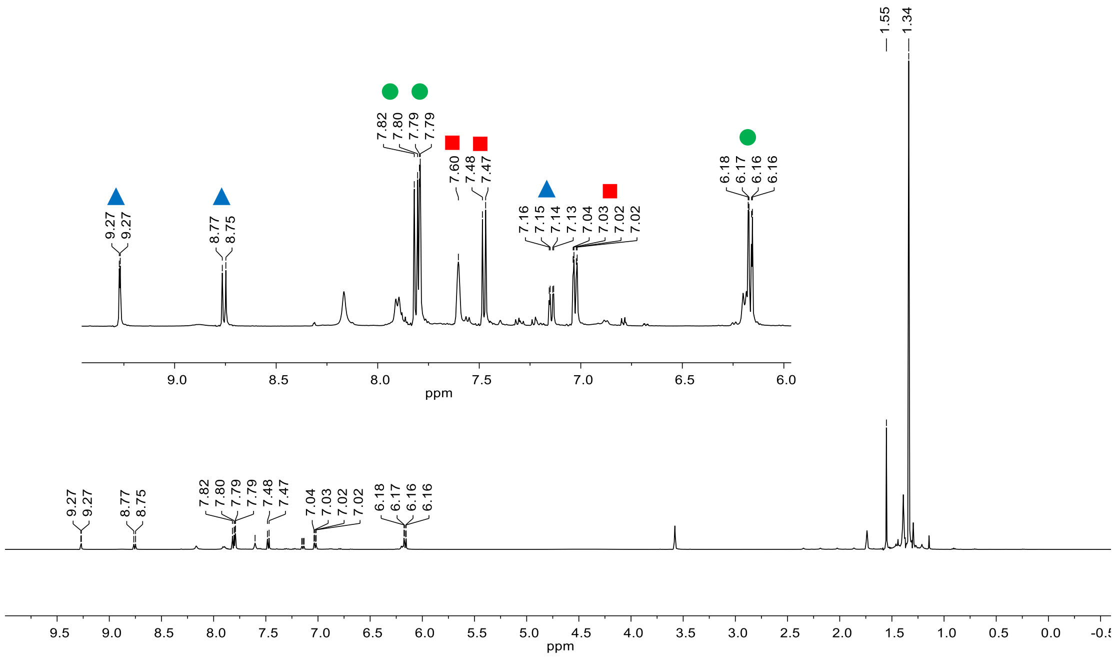

Figure S52: ^{1}H NMR spectrum (500.2 MHz, [D$_8$]THF) recorded on the reaction mixture of the reduction of **1**·THF with sodium metal at room temperature. Marked components: Na$_2$[**1**] (●), Na$_2$[**3**] (▲), Na[**1H**] (■).

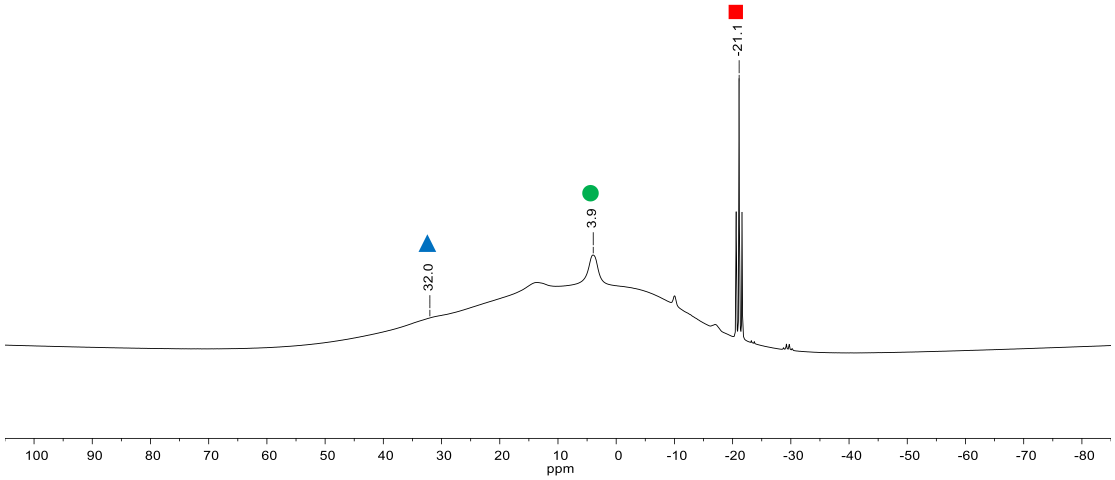

Figure S53: ^{11}B NMR spectrum (160.5 MHz, [D$_8$]THF) recorded on the reaction mixture of the reduction of **1**·THF with sodium metal at room temperature. Marked components: Na$_2$[**1**] (●), Na$_2$[**3**] (▲), Na[**1H**] (■).

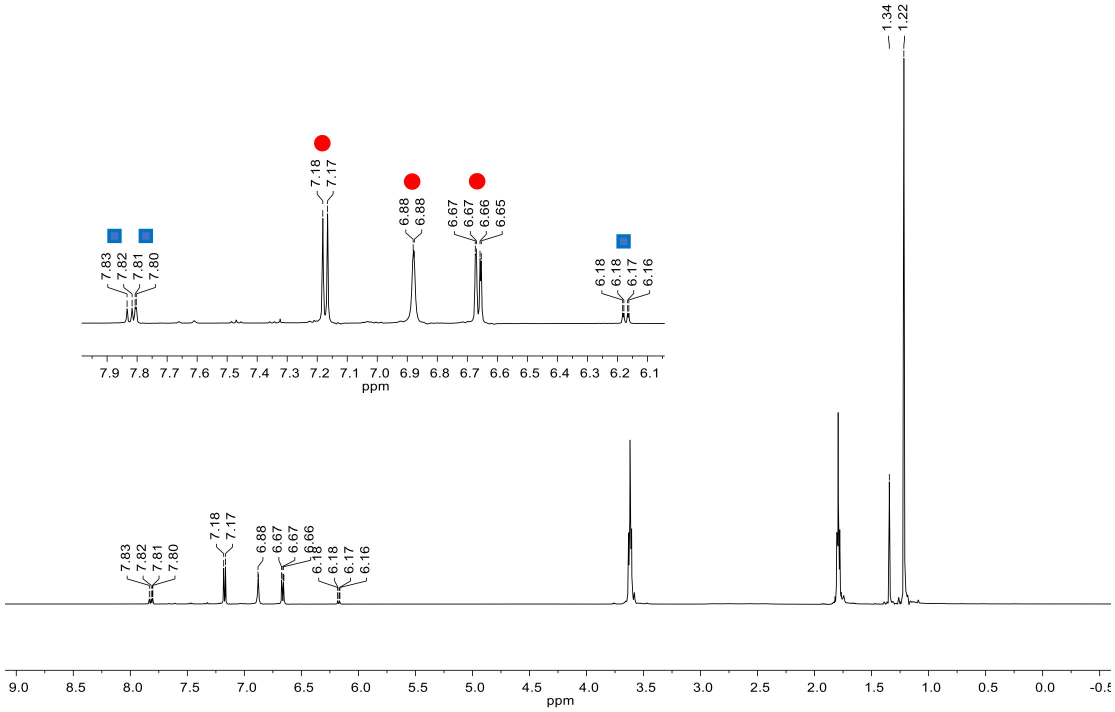

Figure S54: ^{1}H NMR spectrum (500.2 MHz, [D$_8$]THF) recorded on the reaction mixture of the reduction of **1**·THF with sodium metal at only −78 °C. Marked components: Na$_2$[**1**] (■), Na$_2$[**2**] (●).

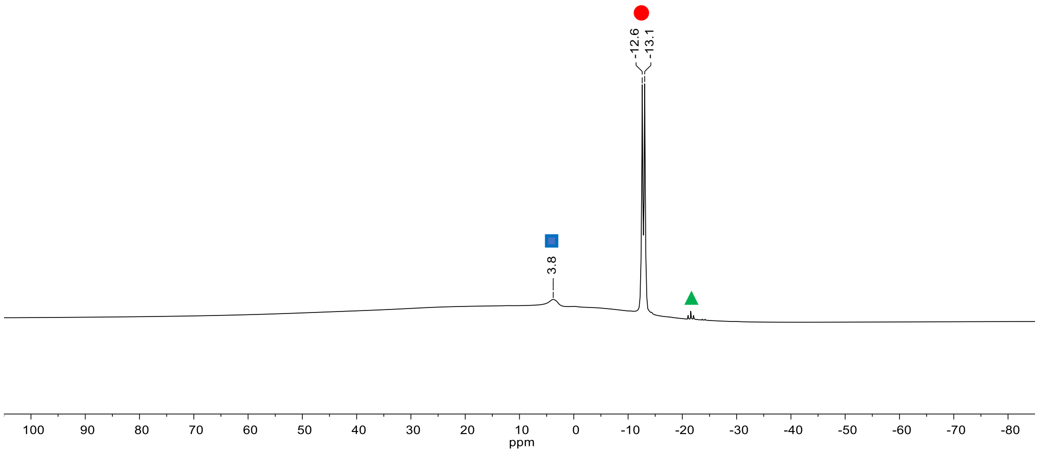

Figure S55: ^{11}B NMR spectrum (160.5 MHz, [D$_8$]THF) recorded on the reaction mixture of the reduction of **1**·THF with sodium metal at only −78 °C. Marked components: Na$_2$[**1**] (■), Na$_2$[**2**] (●), Na[**1H**] (▲; minor component).

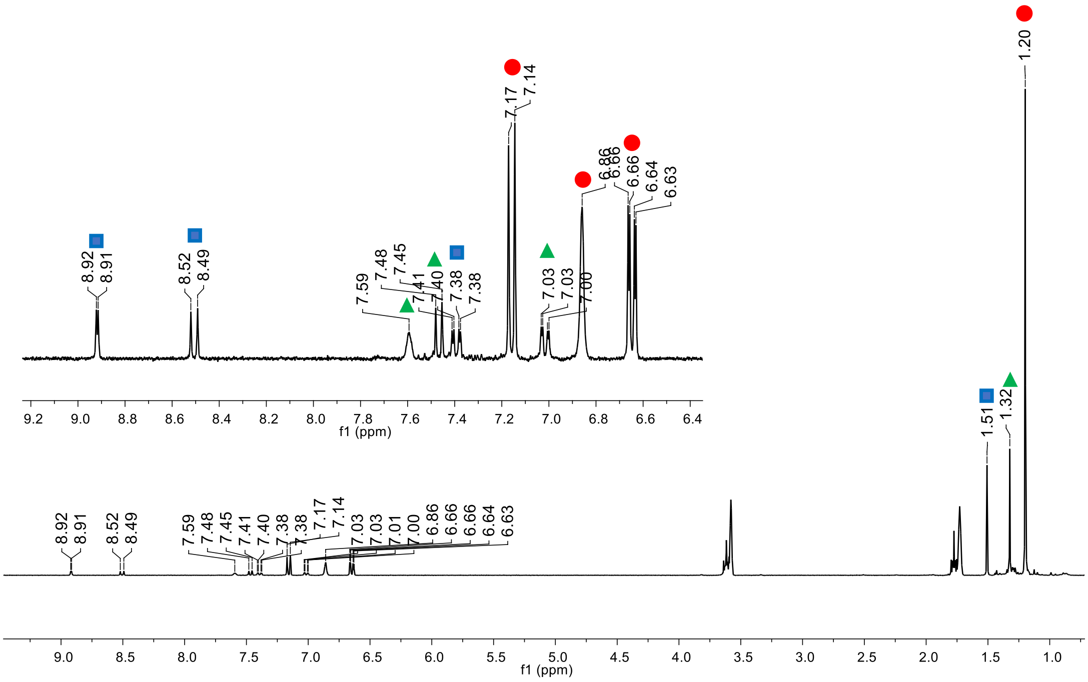

Figure S56: ^{1}H NMR spectrum (300.0 MHz, [D$_8$]THF) recorded on the mixture of Na$_2$[**2**] and **1**·THF. Marked components: Na[**3H**] (■), Na$_2$[**2**] (●), and Na[**1H**] (▲).

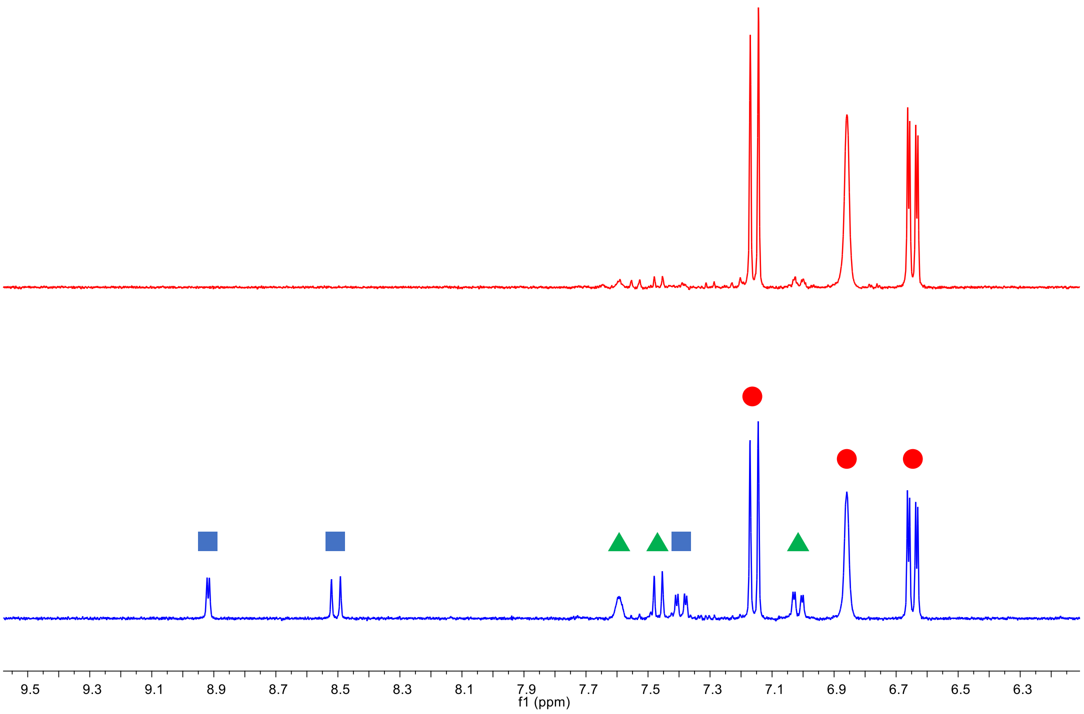

Figure S57: Aromatic and olefinic regions of the ^{1}H NMR spectrum (300.0 MHz, [D$_8$]THF) recorded on Na$_2$[**2**] before (red, top) and after (blue, bottom) addition of 0.25 equiv of **1**·THF. Marked components: Na$_2$[**2**] (●), Na[**3H**] (■), and Na[**1H**] (▲).

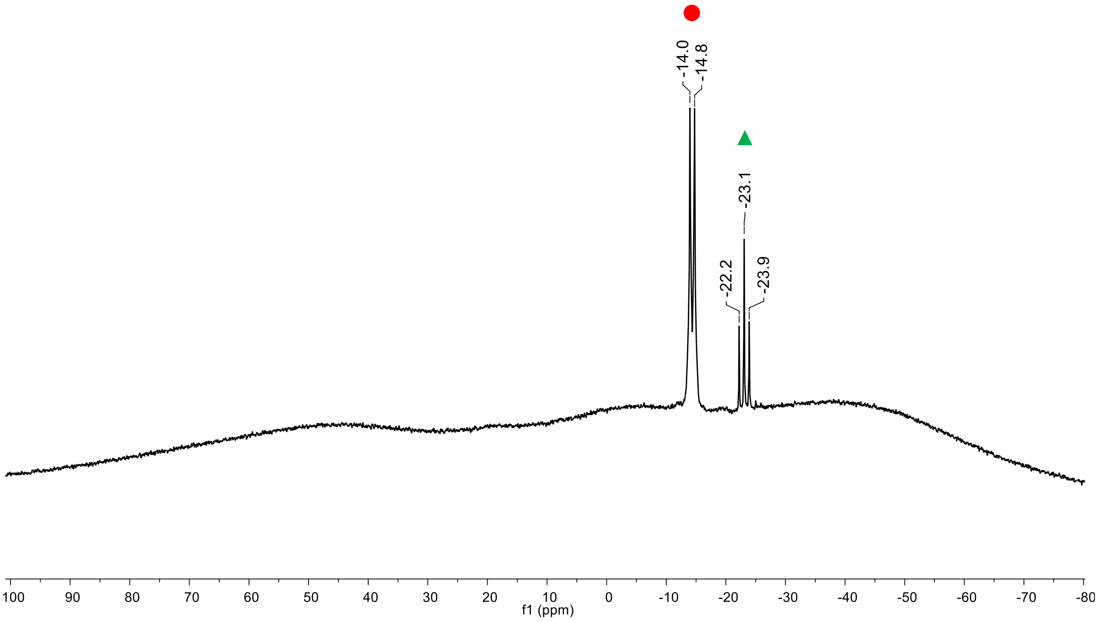

Figure S58: ^{11}B NMR spectrum (160.5 MHz, [D$_8$]THF) recorded on the mixture of Na$_2$[**2**] and **1**·THF. Marked components: Na$_2$[**2**] (●), and Na[**1H**] (▲).

3. X-ray crystal structure analyses of Li_2[1], Na_2[1], Na_2[2]

Data for all structures were collected on a STOE IPDS II two-circle diffractometer with a Genix Microfocus tube with mirror optics using MoK_α radiation (λ = 0.71073 Å). The data were scaled using the frame-scaling procedure in the *X-AREA* program system.[S11] The structures were solved by direct methods using the program *SHELXS* and refined against F^2 with full-matrix least-squares techniques using the program *SHELXL-97*.[S12]

The H atoms bonded to B were isotropically refined in all three structures.

In $[Li_2(thf)_3]$[**1**], one CH_2 group in one thf ligand is disordered over two positions with a site occupation factor of 0.67(4) for the major occupied site. The displacement parameters of the disordered atoms were restrained to an isotropic behavior.

The compound $[Na(thf)_3][Na(thf)]$[**1**] requires no special comments.

In $[Na(thf)_3]_2$[**2**], two *t*Bu-groups are disordered over two positions with site occupation factors of 0.635(7) and 0.785(14) for the major occupied sites. In two thf ligands each, two CH_2 groups are disordered over two positions with site occupation factors of 0.526(16) and 0.67(2) for the major occupied sites. In one thf ligand, one CH_2 group is disordered over two positions with a site occupation factor of 0.78(2) for the major occupied site. The displacement parameters of the disordered atoms and the atoms O71 to C75 (thf) were restrained to an isotropic behavior. The bond lengths and angles of the thf ligand labelled O71 to C75 were restrained to be similar to those in the ligand labelled O91 to C95.

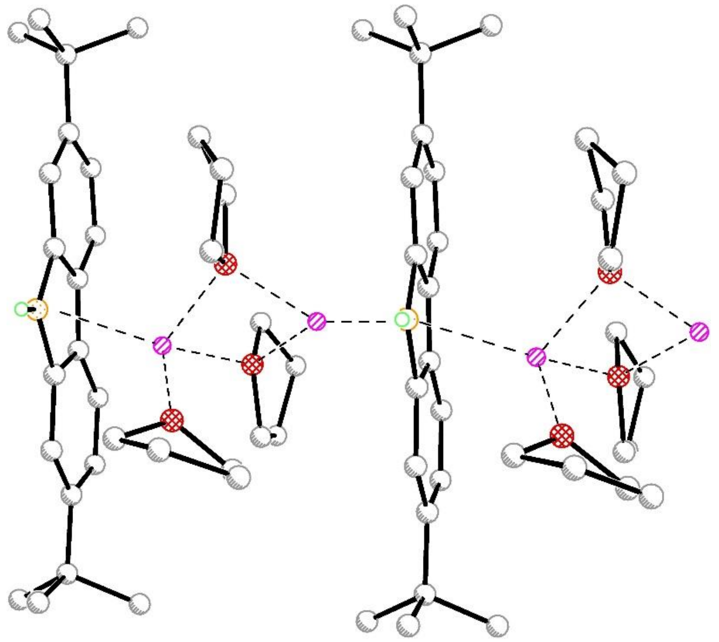

Figure S59: *Description of the crystal structure of [Li$_2$(thf)$_3$][**1**]:* Each side of the C$_4$B ring is coordinated to one Li$^+$ ion. Two thf ligands are bridging two Li$^+$ ions of adjacent borafluorene units so that a coordination polymer is formed. A third thf ligand is just coordinating one of these two Li$^+$ ions.

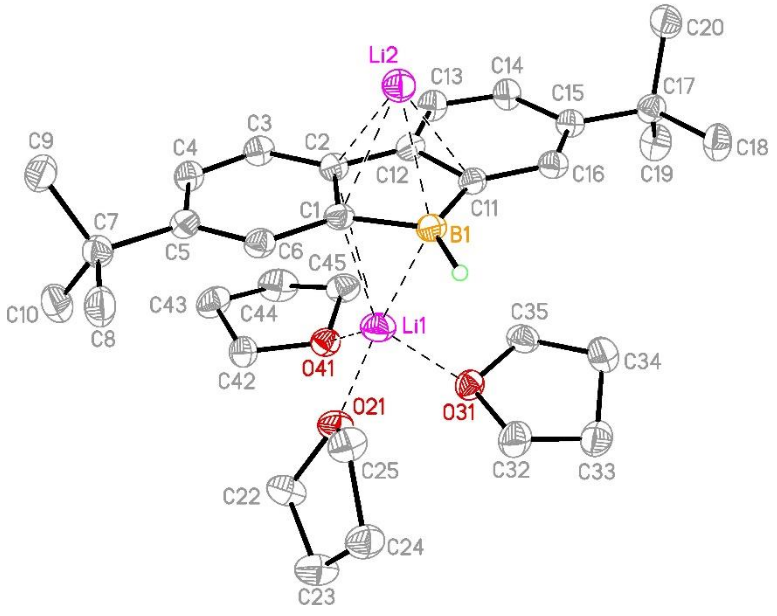

Figure S60: Molecular structure of a section of the coordination polymer [Li$_2$(thf)$_3$][**1**]. Displacement ellipsoids are drawn at the 30% probability level; hydrogen atoms (except for the boron-bonded one) are omitted for clarity. Li(2) was transformed by the symmetry operator –1+x, y, z. Selected atom···atom distances (Å), bond lengths (Å), and bond angles (°): Li1···COG = 2.424(9), Li2···COG = 1.938(9); B1–C1 = 1.525(8), B1–C11 = 1.532(8), B1–H1 = 1.14(9), C1–C2 = 1.475(7), C2–C12 = 1.411(7), C11–C12 = 1.462(7); C1–B1–C11 = 103.8(4), C1–B1–H1 = 125(4), C11–B1–H1 = 130(4); COG = centroid of the C$_4$B ring.

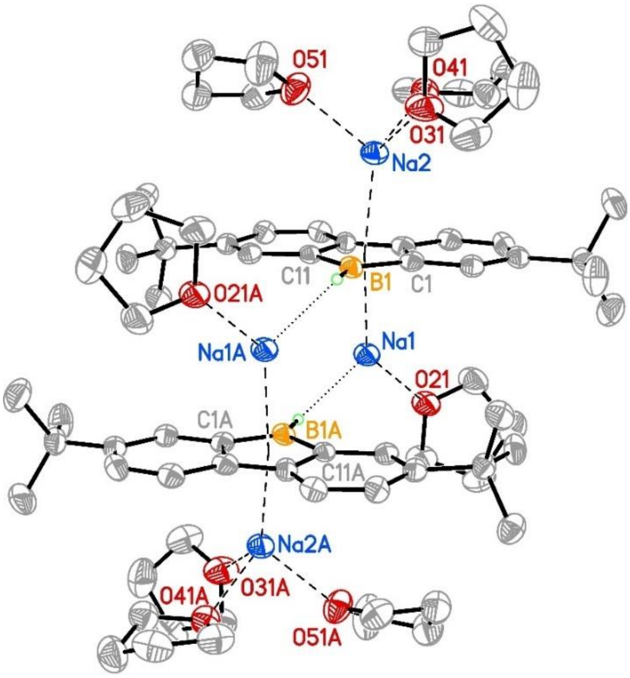

Figure S61: *Description of the crystal structure of [Na(thf)$_3$][Na(thf)][**1**]:* Each side of the C$_4$B ring is coordinated to one Na$^+$ ion. Na2$^+$ carries three thf ligands, Na1$^+$ is coordinated by one thf ligand and the B*H* atom of a second borafluorene unit to generate a centrosymmetric dimer.

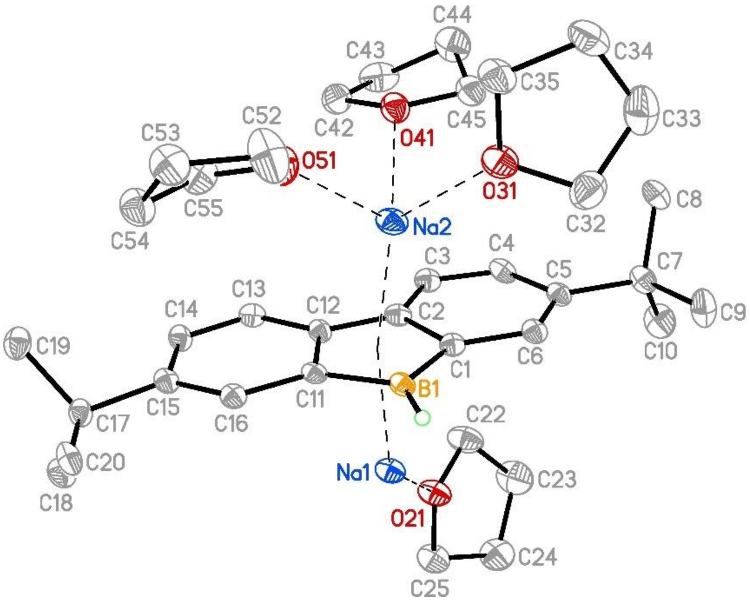

Figure S62: Molecular structure of a monomeric unit of [Na(thf)$_3$][Na(thf)][**1**] in the solid state. Displacement ellipsoids are drawn at the 30% probability level; hydrogen atoms (except for the boron-bonded one) are omitted for clarity. Selected atom···atom distances (Å), bond lengths (Å), and bond angles (°): Na1···COG = 2.432(2), Na1···H1A* = 2.32(4), Na2···COG = 2.501(2); B1–C1 = 1.528(6), B1–C11 = 1.545(6), B1–H1 = 1.13(4), C1–C2 = 1.479(5), C2–C12 = 1.417(6), C11–C12 = 1.473(5); C1–B1–C11 = 104.2(3), C1–B1–H1 =130(2), C11–B1–H1 = 126(2); COG = centroid of the C$_4$B ring. *) H1A was transformed by the symmetry operator 1–x, 1–y, –z.

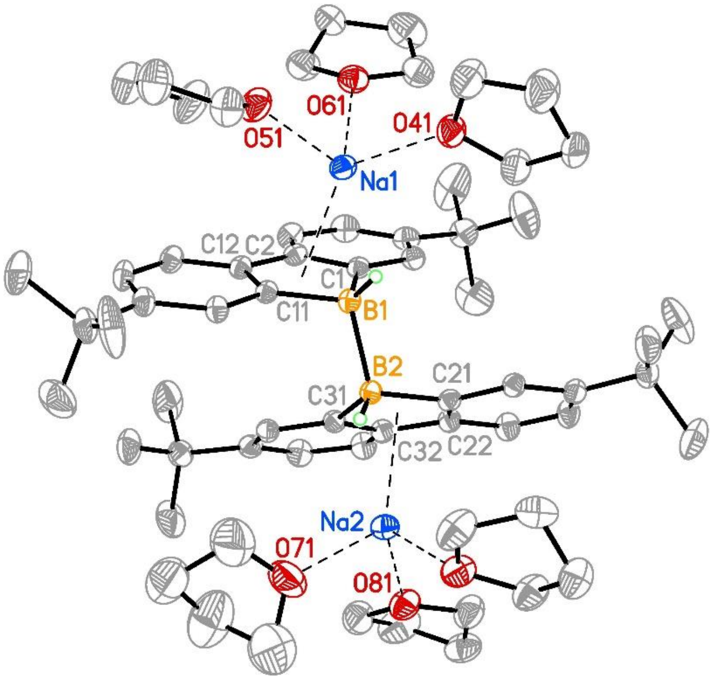

Figure S63: Molecular structure of [Na(thf)$_3$]$_2$[**2**] in the solid state. Displacement ellipsoids are drawn at the 30% probability level; hydrogen atoms (except for the boron-bonded ones) are omitted for clarity. Selected atom···atom distances (Å), bond lengths (Å), and bond angles (°): Na1···COG = 2.6643(14), Na2···COG = 2.5825(16); B1–B2 = 1.822(4), B1–C1 = 1.604(3), B1–C11 = 1.615(3), B1–H1 = 1.20(3), C1–C2 = 1.421(3), C2–C12 = 1.465(3), C11–C12 = 1.418(3), B2–C21 = 1.615(3), B2–C31 = 1.610(3), B2–H2 = 1.15(3), C21–C22 = 1.420(3), C22–C32 = 1.465(4), C31–C32 = 1.422(3); C1–B1–C11 = 99.36(19), C1–B1–B2 = 109.49(18), C11–B1–B2 = 109.55(18), C21–B2–C31 = 99.55(18), C21–B2–B1 = 109.65(18), C31–B2–B1 = 108.56(19); COG = centroids of the C$_4$B rings.

Two borafluorene moieties are connected *via* a B–B bond; one [Na(thf)$_3$]$^+$ ion is bonded to the peripheral side of each C$_4$B ring. The dianion [**2**]$^{2–}$ is remarkable, because the electrostatic repulsion between the two associated negative charges is expected to destabilize the B−B single bond, which, in [Na(thf)$_3$]$_2$[**2**], is expanded to a length of 1.822(4) Å (Figure S63).

Table S1: Selected crystallographic data for [Li_2(thf)$_3$][**1**] and [Na(thf)$_3$][Na(thf)][**1**].

	[Li_2(thf)$_3$][**1**]	[Na(thf)$_3$][Na(thf)][**1**]
CCDC	1963735	1963736
formula	$C_{32}H_{49}BLi_2O_3$	$C_{72}H_{114}B_2Na_4O_8$
M_r	506.40	1221.21
T (K)	173(2)	173(2)
radiation, λ (Å)	0.71073	0.71073
crystal system	monoclinic	triclinic
space group	$P2_1/c$	P-1
a (Å)	7.0447(3)	9.4875(10)
b (Å)	13.7119(9)	13.5396(15)
c (Å)	30.7906(13)	15.0072(18)
α (°)	90	76.783(9)
β (°)	91.917(3)	79.830(9)
γ (°)	90	74.040(8)
V (Å^3)	2972.6(3)	1791.0(4)
Z	4	1
D_{calcd} (g cm^{-3})	1.132	1.132
F(000)	1104	664
μ (mm^{-1})	0.068	0.091
crystal size (mm)	0.210 × 0.120 × 0.050	0.290 × 0.120 × 0.080
crystal shape, color	plate, black	plate, orange
reflections collected	21581	19940
independent reflections	5246	6307
R_{int}	0.0708	0.0668
data / restraints / parameters	5246 / 12 / 357	6307 / 0 / 392
R_1, wR_2 ($I > 2\sigma(I)$)	0.1130, 0.2976	0.0966, 0.1777
R_1, wR_2 (all data)	0.1501, 0.3222	0.1424, 0.1976
GOF on F^2	1.157	1.157
Largest difference peak and hole (e Å^{-3})	0.416, –0.332	0.300, –0.273

Table S2: Selected crystallographic data for $[Na(thf)_3]_2$[**2**].

	$[Na(thf)_3]_2$[**2**]
CCDC	1963737
formula	$C_{64}H_{98}B_2Na_2O_6$
M_r	1031.02
T (K)	173(2)
radiation, λ (Å)	0.71073
crystal system	monoclinic
space group	$P2_1/n$
a (Å)	13.5093(5)
b (Å)	19.2223(5)
c (Å)	23.9947(8)
α (°)	90°
β (°)	94.337(3)
γ (°)	90
V (Å^3)	6213.1(4)
Z	4
D_{calcd} (g cm^{-3})	1.102
F(000)	2248
μ (mm^{-1})	0.080
crystal size (mm)	0.260 × 0.260 × 0.230
crystal shape, color	block, yellow
reflections collected	62160
independent reflections	12097
R_{int}	0.0510
data / restraints / parameters	12097 / 182 / 779
R_1, wR_2 ($I > 2\sigma(I)$)	0.0791, 0.2239
R_1, wR_2 (all data)	0.1032, 0.2514
GOF on F^2	1.025
Largest difference peak and hole (e Å^{-3})	1.641, –0.560

4. Electronic structure of Na_2[1]

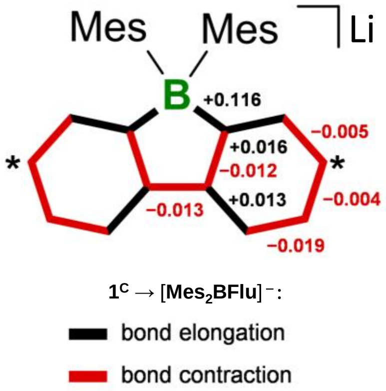

Figure S64: Differences between selected bond lengths [Å] of **1**^{C} and [Li(thf)$_4$][(Mes)$_2$BFlu][S13] (BFlu = borafluorenyl). Carbon atoms marked with asterisks bear *t*Bu substituents.

An inspection of the ^{13}C{^{1}H} NMR spectrum of Li[**1H**] revealed that the changes observed in the NMR spectra upon going from BrBFlu to Na_2[**1**] cannot be brought about by occupying the vacant boron p_z orbital with the *localized* electron pair of a negatively charged Lewis base (Figure S64).

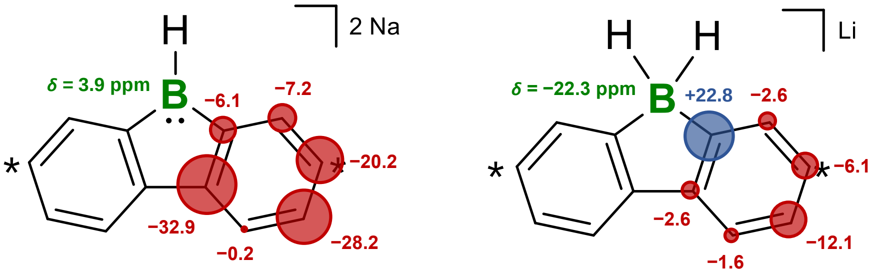

Na_2[**1**]

Li[**1H**]

Figure S65: Differences between selected ^{13}C NMR shift values [ppm] of 2,7-di-*tert*- butyl-9-bromo-9-borafluorene (BrBFlu, C_6D_6)[S1] and [Na]$_2$[**1**] ([D_8]THF, left), or BrBFlu (C_6D_6) and Li[**1H**] ([D_8]THF, right).[S6] The ^{11}B NMR shift values are depicted in green. Carbon atoms marked with asterisks bear *t*Bu substituents. The shielding of a specific arene carbon atom depends linearly on the corresponding π-electron density at this position and its ^{13}C shift remains largely unaffected from the solvent employed: C. Hoffend, M. Diefenbach, E. Januszewski, M. Bolte, H.-W. Lerner, M. C. Holthausen, M. Wagner, *Dalton Trans.* **2013**, *42*, 13826-13837 and references cited therein.

5. Computational details

DFT calculations were carried out with the Gaussian program package.[S14] The B3LYP hybrid functional[S15] was used and combined with the D3 atom-pairwise dispersion correction devised by Grimme.[S16] Geometry optimizations and harmonic frequency calculations were computed under gas-phase conditions with the TZVP basis set.[S17] All stationary points reported were characterized as minima or first order saddle points by eigenvalue analysis of the diagonalized Hessians. The graphics were produced with Avogadro 1.1.1 and POV-Ray 3.7.0.

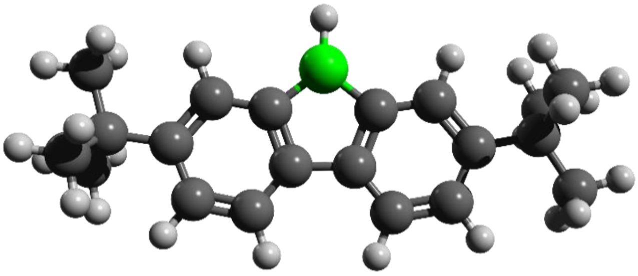

1^{C}

C	−0,72508	−0,42072	−0,00038
C	0,72863	−0,41517	0,00300
C	1,18461	0,88667	−0,00345
B	−0,01638	1,84642	−0,00489
C	−1,20482	0,87163	−0,00422
C	−2,55707	1,14605	−0,00670
C	−3,47239	0,06701	−0,00440
C	−2,96183	−1,26934	−0,00037
C	−1,58002	−1,51003	0,00375
C	1,61598	−1,48605	0,00238
C	2,99070	−1,21548	0,00018
C	3,46501	0,13081	0,00440
C	2,52850	1,18754	−0,00253
C	−4,97368	0,37188	−0,00600
C	−5,32887	1,19428	1,24902
C	−5,31964	1,18586	−1,27512
C	−5,82579	−0,91157	−0,00774
C	4,97303	0,40830	0,00050
C	5,60004	−0,21218	1,26417
C	5,60290	−0,21022	−1,26359
C	5,29124	1,92443	0,00243
H	−0,01962	3,02716	−0,00866
H	−2,88701	2,17325	−0,00926
H	−3,60775	−2,13075	0,00328
H	−1,20204	−2,52300	0,00777
H	1,25701	−2,50260	0,00160
H	3,67733	−2,04779	0,00042
H	2,80561	2,23065	−0,00172
H	−4,78572	2,16192	1,27783
H	−5,06611	0,62653	2,16845
H	−6,41553	1,42282	1,27231
H	−4,77560	2,15348	−1,30613
H	−6,40586	1,41584	−1,30773
H	−5,05025	0,61289	−2,18923
H	−5,61497	−1,51544	0,90169
H	−5,60903	−1,52220	−0,91154
H	−6,90899	−0,67060	−0,01219
H	5,45185	−1,31203	1,29475
H	5,13565	0,22323	2,17688
H	6,69307	−0,01721	1,29567
H	5,45460	−1,30932	−1,29528
H	6,69576	−0,01496	−1,29141
H	5,14116	0,22671	−2,17479
H	4,86482	2,41113	0,90900
H	4,86824	2,41309	−0,90293
H	6,38424	2,11034	0,00494

6. References

[S1] A. Hübner, M. Diefenbach, M. Bolte, H. W. Lerner, M. C. Holthausen, M. Wagner, *Angew. Chem. Int. Ed.* **2012**, *51*, 12514–12518.

[S2] T. Kaese, T. Trageser, H. Budy, M. Bolte, H.-W. Lerner, M. Wagner, *Chem. Sci.* **2018**, *9*, 3881–3891.

[S3] G. R. Fulmer, A. J. M. Miller, N. H. Sherden, H. E. Gottlieb, A. Nudelman, B. M. Stoltz, J. E. Bercaw, K. I. Goldberg, *Organometallics* **2010**, *29*, 2176–2179.

[S4] T. Kaese, A. Hübner, M. Bolte, H. W. Lerner, M. Wagner, *J. Am. Chem. Soc.* **2016**, *138*, 6224–6233.

[S5] Depending on the quality of the alkali metal employed, it can be advisable to continue stirring for 2 d (in total).

[S6] A. Hübner, M. Bolte, H. W. Lerner, M. Wagner, *Angew. Chem. Int. Ed.* **2014**, *53*, 10408–10411.

[S7] We initially performed the reaction with excess Me_3SnCl and obtained a complex product mixture. To be sure to avoid any excess of Me_3SnCl as a result of weighing errors in the present case, we used 0.9 rather than 1 equiv.

[S8] T. N. Mitchell, J. *Organomet. Chem.* **1974**, *70*, C1–C2.

[S9] A. G. Lichtscheidl, M. T. Janicke, B. L. Scott, A. T. Nelson, J. L. Kiplinger, *Dalton Trans.* **2015**, *44*, 16156–16163.

[S10] Li[**1H**][S6], K[**1H**][S4], Li[**3H**] (T. Kaese, H. Budy, M. Bolte, H.-W. Lerner, M. Wagner, *Angew. Chem. Int. Ed.* **2017**, *56*, 7546-7550), K[**3H**][S4], and Li_2[**3**][S6]are known; the NMR resonances of Na[**1H**], Na[**3H**], and Na[**3**] were assigned by analogy.

[S11] Stoe & Cie, *X-AREA. Diffractometer control program system*. Stoe & Cie, Darmstadt, Germany, **2002**.

[S12] G. M. Sheldrick, *Acta Crystallogr. Sect. A Found. Crystallogr.* **2008**, *64*, 112–122.

[S13] J. Radtke, S. Mellerup, M. Bolte, H.-W. Lerner, S. Wang, M. Wagner, *Org. Lett.* **2018**, *20*, 3966-3970.

[S14] Gaussian 09, Revision D.01, M. J. Frisch, G. W. Trucks, H. B. Schlegel, G. E. Scuseria, M. A. Robb, J. R. Cheeseman, G. Scalmani, V. Barone, B. Mennucci, G. A. Petersson, H. Nakatsuji, M. Caricato, X. Li, H. P. Hratchian, A. F. Izmaylov, J. Bloino, G. Zheng, J. L. Sonnenberg, M. Hada, M. Ehara, K. Toyota, R. Fukuda, J. Hasegawa, M. Ishida, T. Nakajima, Y. Honda, O. Kitao, H. Nakai, T. Vreven, J. A. Montgomery, Jr., J. E. Peralta, F. Ogliaro, M. Bearpark, J. J. Heyd, E. Brothers, K. N. Kudin, V. N. Staroverov, T. Keith, R. Kobayashi, J. Normand, K. Raghavachari, A. Rendell, J. C. Burant, S. S. Iyengar, J. Tomasi, M. Cossi, N. Rega, J. M. Millam, M. Klene, J. E. Knox, J. B. Cross, V. Bakken, C. Adamo, J. Jaramillo, R. Gomperts, R. E. Stratmann, O. Yazyev, A. J. Austin, R. Cammi, C. Pomelli, J. W. Ochterski, R. L. Martin, K. Morokuma, V. G. Zakrzewski, G. A. Voth, P. Salvador, J. J. Dannenberg, S. Dapprich, A. D. Daniels, O. Farkas, J. B. Foresman, J. V. Ortiz, J. Cioslowski, and D. J. Fox, Gaussian, Inc., Wallingford, CT, USA, **2013**.

[S15] a) A. D. Becke, *Phys. Rev. A* **1988**, 38, 3098–3100. (b) C. Lee, W. Yang, R. G. Parr, *Phys. Rev. B* **1988**, 37, 785–789. (c) P. J. Stephens, F. J. Devlin, C. F. Chabalowski, M. J.Frisch, *J. Phys. Chem.* **1994**, 98, 11623–11627. (d) A. D. Becke, *J. Chem. Phys.* **1993**, 98, 5648–5652.

[S16] S. Grimme, J. Antony, S. Ehrlich, H. Krieg, *J. Chem. Phys.* **2010**, *132*, 154104.

[S17] A. Schäfer, C. Huber, R. Ahlrichs, *J. Chem. Phys.* **1994**, *100*, 5829–5835.